Telomere Shortening and Cellular Senescence Induced by Oxalate

and Nephrolithiasis Urine in HK-2 cells

Miss Kamonchanok Chuenwisad

จุฬาลงกรณ์มหาวิทยาลัย
CHULALONGKORN UNIVERSITY

A Thesis Submitted in Partial Fulfillment of the Requirements

for the Degree of Master of Science in Medical Biochemistry

Department of Biochemistry

FACULTY OF MEDICINE

Chulalongkorn University

Academic Year 2020

การหดสั้นลงของเทโลเมียร์และการแก่ของเซลล์ที่ถูกเหนี่ยวนำด้วยออกซาเลต
และปัสสาวะผู้ป่วยโรคนิ่วไตในเซลล์เยื่อบุท่อไต

น.ส.กมลชนก ชื่นวิเศษ

Thesis Title   Telomere Shortening and Cellular Senescence Induced by Oxalate and Nephrolithiasis Urine in HK-2 cells

By   Miss Kamonchanok Chuenwisad

Field of Study   Medical Biochemistry

Thesis Advisor   Assistant Professor CHANCHAI BOONLA, Ph.D.

Thesis Co Advisor   Assistant Professor Monpichar Srisa-Art, Ph.D.

Accepted by the FACULTY OF MEDICINE, Chulalongkorn University in Partial Fulfillment of the Requirement for the Master of Science

.... Dean of the FACULTY OF MEDICINE

(Professor SUTTIPONG WACHARASINDHU, M.D.)

THESIS COMMITTEE

.... Chairman

(Professor Sittisak Honsawek, M.D.)

.... Thesis Advisor

(Assistant Professor CHANCHAI BOONLA, Ph.D.)

.... Thesis Co-Advisor

(Assistant Professor Monpichar Srisa-Art, Ph.D.)

.... Examiner

(Naphat Chantaravisoot, Ph.D.)

.... External Examiner

(Assistant Professor Supranee Kongkham, Ph.D.)

กมลชนก ชื่นวิเศษ : การหดสั้นลงของเทโลเมียร์และการแก่ของเซลล์ที่ถูกเหนี่ยวนำด้วยออกซาเลต และปัสสาวะผู้ป่วยโรคนิ่วไตในเซลล์เยื่อบุท่อไต. (Telomere Shortening and Cellular Senescence Induced by Oxalate and Nephrolithiasis Urine in HK-2 cells) อ.ที่ปรึกษาหลัก : ผศ. ดร.ชาญชัย บุญหล้า, อ.ที่ปรึกษาร่วม : ผศ. ดร.มนพิชา ศรีสะอาด

โรคนิ่วไตเป็นปัญหาระบบทางเดินปัสสาวะที่พบได้ทั่วโลก โดยเฉพาะในเขตร้อน รวมทั้งประเทศไทย โดยเป็นที่ทราบกันดีว่าการก่อตัวของก้อนนิ่วมีหลายสาเหตุ และอายุที่เพิ่มขึ้นยังเพิ่มความเสี่ยงของการเกิดก้อนนิ่วอีกด้วย ชนิดของนิ่วไตที่พบมากที่สุดคือ นิ่วแคลเซียมออกซาเลต (CaOx) ซึ่งเกิดจากการขับออกของออกซาเลตในปัสสาวะที่เพิ่มขึ้น และมีการสร้างผลึกแคลเซียมออกซาเลตโมโนไฮเดรต (COM) มากขึ้น โดยทั้งออกซาเลต และ COM สามารถเหนี่ยวนำให้เกิดการสร้างอนุมูลอิสระ (ROS) และทำให้เกิดภาวะเครียดออกซิเดชั่น ยิ่งไปกว่านั้น ผู้ป่วยโรคนิ่วชนิด CaOx ยังมีภาวะเครียดออกซิเดชั่นเพิ่มสูงขึ้นกว่าปกติอีกด้วย ในการศึกษานี้ ผู้วิจัยได้ทำการศึกษาการเหนี่ยวนำให้เกิดการแก่ของเซลล์ และการหดสั้นลงของเทโลเมียร์ผ่านทางภาวะเครียดออกซิเดชั่นใน HK-2 cells ด้วยออกซาเลต COM และปัสสาวะจากผู้ป่วยโรคนิ่วชนิด CaOx (KS) จำนวน 5 ราย โดยทำการเลือกปัสสาวะของอาสาสมัครที่ไม่เป็นนิ่ว (NS) จำนวน 5 ราย ที่มีอายุและเพศใกล้เคียงกัน เพื่อนำมาใช้เป็นปัสสาวะควบคุม โดยในการทดลอง HK-2 cells ถูกเหนี่ยวนำด้วย H_2O_2 (ใช้เป็นตัวแทนของ ROS) ออกซาเลต COM และตัวอย่างปัสสาวะ (10% v/v) เป็นเวลา 72 ชั่วโมง ผลการศึกษาพบว่า จำนวนเซลล์แก่ (SA-βgal positive cells) เพิ่มสูงขึ้นอย่างมีนัยสำคัญทางสถิติในกลุ่มที่เหนี่ยวนำด้วย H_2O_2 ออกซาเลต COM และปัสสาวะในกลุ่ม KS เมื่อเทียบกับ ปัสสาวะในกลุ่ม NS และ untreated control ในส่วนของภาวะเครียดออกซิเดชั่น ซึ่งตรวจวัดจากการเพิ่มขึ้นของระดับโปรตีนคาร์บอนิล และการลดลงของความสามารถในการต้าน ROS ในกลุ่มที่เหนี่ยวนำด้วย H_2O_2 ออกซาเลต COM และปัสสาวะในกลุ่ม KS เพิ่มสูงขึ้นอย่างมีนัยสำคัญทางสถิติเมื่อเทียบกับ untreated control และปัสสาวะในกลุ่ม NS การแสดงออกของโปรตีน p16 มีการเพิ่มขึ้นอย่างเห็นได้ชัดในกลุ่มที่เหนี่ยวนำด้วย H_2O_2 ออกซาเลต COM และปัสสาวะในกลุ่ม KS เมื่อเทียบกับ untreated control และปัสสาวะในกลุ่ม NS ความยาวเทโลเมียร์สัมพัทธ์ลดลงอย่างมีนัยสำคัญทางสถิติในกลุ่มที่เหนี่ยวนำด้วย H_2O_2 ออกซาเลต COM และปัสสาวะในกลุ่ม KS เมื่อเทียบกับ untreated control และปัสสาวะในกลุ่ม NS และการแสดงออกระดับ mRNA ของยีน TRF1 TRF2 และ POT1 ลดลงอย่างมีนัยสำคัญทางสถิติในกลุ่มที่เหนี่ยวนำด้วย H_2O_2 ออกซาเลต COM และปัสสาวะในกลุ่ม KS เมื่อเทียบกับ untreated control และปัสสาวะในกลุ่ม NS จากผลการศึกษาที่ได้สามารถสรุปได้ว่า การศึกษานี้เป็นการศึกษาแรกที่แสดงให้เห็นว่า ออกซาเลต COM ปัสสาวะในกลุ่ม KS สามารถเหนี่ยวนำให้เกิดการแก่ของเซลล์และการหดสั้นลงของเทโลเมียร์ในเซลล์เยื่อบุท่อไต โดยการเหนี่ยวนำให้เกิดการแก่ของเซลล์นี้ผ่านทางภาวะเครียดออกซิเดชั่นและมีความสัมพันธ์กับการแสดงออกที่เพิ่มขึ้นของ p16 และการแสดงออกที่ลดลงของยีน shelterin complex ผลการศึกษานี้ชี้แนะว่าการแก่ของเซลล์และการหดสั้นลงของเทโลเมียร์ผ่านทางภาวะเครียดออกซิเดชั่นในเซลล์เยื่อบุท่อไตที่ถูกเหนี่ยวนำด้วยสารก่อนิ่ว โดยเฉพาะออกซาเลต และ COM น่าจะเป็นหนึ่งในกลไกส่งเสริมการเกิดโรคนิ่วไตชนิด CaOx

สาขาวิชา	ชีวเคมีทางการแพทย์	ลายมือชื่อนิสิต ....
ปีการศึกษา	2563	ลายมือชื่อ อ.ที่ปรึกษาหลัก ....
		ลายมือชื่อ อ.ที่ปรึกษาร่วม ....

6174091030 : MAJOR MEDICAL BIOCHEMISTRY

KEYWORD: Kidney stone / Nephrolithiasis / ROS / Oxidative stress / Telomere shortening / Shelterin / Senescence / SIPS / STASIS

Kamonchanok Chuenwisad : Telomere Shortening and Cellular Senescence Induced by Oxalate and Nephrolithiasis Urine in HK-2 cells. Advisor: Asst. Prof. CHANCHAI BOONLA, Ph.D. Co-advisor: Asst. Prof. Monpichar Srisa-Art, Ph.D.

Kidney stone disease is a common urologic problem worldwide, especially in the tropics such as Thailand. It is known as a multifactorial condition, and aging increases the risk of stone development. The major type of stones is calcium oxalate (CaOx), and its formation is driven by increased urinary oxalate excretion and calcium oxalate monohydrate (COM) crystallization. Both oxalate and COM are known to induce reactive oxygen species (ROS) production and cause oxidative stress. Furthermore, patients with CaOx stone have increased extent of oxidative stress. In this study, we investigated the induction of cellular senescence and telomere shortening through oxidative stress by oxalate, COM and urine obtained from CaOx kidney stone (KS) patients (n=5) in HK-2 cells. Five urine samples from the age- and sex-matched non-stone (NS) subjects were used as urine control. HK-2 cells were treated with H_2O_2 (representative of ROS), oxalate, COM and urine samples (10% v/v) for 72 h. The result shown that the number of senescent (SA-βgal positive) cells were significantly higher in H_2O_2-, oxalate-, COM- and KS urine-treated conditions than that of the NS urine-treated and untreated conditions. Oxidative stress, indicated by increased protein carbinyl level and decreased total antioxidant capacity, was significantly increased in cells treated with H_2O_2, oxalate, COM and KS urine relative to the untreated control and NS urine. The expression of p16 protein was clearly increased in the H_2O_2-, oxalate-, COM- and KS urine-treated cells compared with the untreated control and NS urine-treated cells. In contrast, relative telomere length was significantly decreased in the H_2O_2-, oxalate-, COM- and KS urine-treated cells compared with the untreated control and NS urine-treated cells. Expression of TRF1, TRF2 and POT1 mRNAs was significantly lower in cells treated with H_2O_2, oxalate, COM and KS urine than that of the untreated control and NS urine. In conclusion, this is the first study showing that oxalate, COM and KS urine induce cellular senescence and telomere shortening in renal proximal tubular cells. This senescent induction is mediated through oxidative stress and associated with upregulation of p16 and downregulation of shelterin complex genes. Our findings suggest that oxidative stress-mediated senescence and telomere shortening in renal proximal tubular cells induced by lithogenic factors, particularly oxalate and COM, may contribute to the development of CaOx kidney stone disease.

Field of Study:	Medical Biochemistry	Student's Signature	
Academic Year:	2020	Advisor's Signature	
		Co-advisor's Signature	

ACKNOWLEDGEMENTS

จุฬาลงกรณ์มหาวิทยาลัย

CHULALONGKORN UNIVERSITY

TABLE OF CONTENTS

Introduction

The title

(ภาษาไทย):   การหดสั้นลงของเทโลเมียร์และการแก่ของเซลล์ที่ถูกเหนี่ยวนำด้วยออกซาเลต และ
ปัสสาวะผู้ป่วยโรคนิ่วไตในเซลล์เยื่อบุท่อไต

(English):   Telomere Shortening and Cellular Senescence Induced by Oxalate and
Nephrolithiasis Urine in HK-2 cells

1.   Background and Rationales

Kidney stone disease or nephrolithiasis is a common urological disease worldwide, especially in the tropical areas. In Thailand, kidney stone disease is prevalent, reported up to 16.9% in the Northeast (1). The disease is frequently found in men more than women (2). Etiology of stone disease is multifactorial. Predisposition of stone formation increases with age (3). Kidney stone is highly recurrent and causes decline of kidney function. It increases risk of chronic kidney disease (CDK), and eventually death is a consequence (4).

Kidney stone compositions are heterogenous. Types of stones are classified by types of mineral composition including calcium oxalate (CaOx), calcium phosphate (CaP), magnesium ammonium phosphate (MAP) or struvite or infection stone, uric acid (UA) and cystine stones (5). CaOx is the most common stone found up to 80%. Formation of CaOx stone is largely promoted by dietary risk factors such as low fluid intake, high consumption of stone promoters, especially oxalate, and low consumption of stone inhibitors, specifically citrate. Increased urinary level of stone promoters and decreased stone inhibitors lead to urine supersaturation and crystallization of CaOx in

urine that drive stone formation (6). CaOx crystals, particularly calcium oxalate monohydrate (COM) induces generation of reactive oxygen species (ROS) leading to oxidative stress. ROS is known to cause damage to cellular biomolecules, trigger cellular senescence and at high dose induce apoptosis (7). Evidence reports that elderly aged over 60 years old have decreased renal mass and repairing capability, and increased renal tubular cell senescence (8).

Cellular senescence induced by oxidative stress is associated with telomere attrition (9). Telomeres are the ends of mammal chromosomes that are composed of TTAGGG repeats and normally associated with the protein complex (shelterin) forming the T-loop structure with the ends of chromosome to protect the ends of chromosomes from DNA strand breaks and DNA damage response pathway (10). In human somatic cells, the length of telomeres is decreased every round of cell division due to the lack of telomerase enzyme for extending the length of telomeres. When telomeres are critically shorten, it results in cell cycle arrest and the cell enters into the senescent state (11). The accumulation of ROS and increased oxidative stress cause the rapid shortening of telomeres because the telomeric regions are rich in guanine (G) content that is highly susceptible for oxidative modification. The 8-oxoguanine (8-oxo-G) lesions are remarkedly produced under the oxidative stress condition. Accumulation of these oxidative lesions causes improper function of shelterin complex resulting in DNA strand breaks and shortening of telomeres (12). When telomeres are critically shorten, the telomere binding proteins are disrupted and the DNA damage response is activated that further leads to senescence and ultimately apoptosis (13). The other mechanism of telomere shortening in ROS-induced cellular senescence involves downregulation of shelterin protein complex. In previous studies showed that fibroblasts and human hepatocytes treated with H_2O_2 exhibited stress-induced premature senescence (SIPS) and decreased expression of shelterin protein complex (RAP1, TRF1, TRF2 and POT1), and that led to telomere shortening (14, 15). In clinical setting, several aging/oxidative stress-associated diseases are found to have

telomere attrition, such as, cardiovascular diseases, neurodegenerative diseases and chronic kidney diseases (16).

Cellular senescence is the state of cell cycle arrest characterized by loss of cell proliferation, but still viable. The well-recognized marker of the senescence cells is lysosomal β-galactosidase enzyme that is normally detected at pH 4 in normal cells, but it is detected at pH nearly 6 in senescent cells (17). The other well-known senescent marker is p16^{INK4a}. The p16 protein specifically inhibits the activation of cyclin D-Cdk4/6 and is associated with pRB activation leading to cell cycle arrest and senescence. There are two common types of cellular senescence. One is replicative senescence, and the other is stress-induced premature senescence (SIPS) or aberrant signaling-induced senescence (STASIS). Replicative senescence is directly caused by telomere shortening that is beneficial for cancer suppression. SIPS or STASIS is the premature senescence that triggers by stress factors including ROS and oxidative stress. The key distinctive proteins of the replicative and STASIS pathways are p53 and p16^{INK4a}, respectively (18).

The effect of oxidative stress in induction of renal cell senescence in CDK patients is widely studied, but there is none in nephrolithiasis. To our knowledge, telomere erosion and renal cell senescence induced by lithogenic factors have not been investigated. We hypothesized that high level of oxalate and CaOx crystallization in urine of nephrolithiasis patients were capable of inducing ROS generation and oxidative stress in the renal tubular cells, and consequently caused telomere attrition and cellular senescence.

In this study, the induction of telomere shortening and senescence by oxalate, CaOx crystals, urine from kidney stone (KS) patients and urine from non-stone (NS) subjects in human kidney (HK-2) cells were investigated. Changes in expression of p16 and shelterin protein (TRF1, TRF2 and POT1) by these lithogenic factors were determined.

2. Keywords

Kidney stone, Nephrolithiasis, ROS, Oxidative stress, Telomere shortening, Shelterin, Senescence, SIPS, STASIS

3. Research questions

1. Whether oxalate, COM and urine obtained from KS patients induced telomere shortening and senescence in renal proximal tubular epithelial cells (HK-2 cells) through oxidative stress.

2. Whether the induction of telomere shortening and senescence by oxalate, COM and KS urine in HK-2 cells was mediated through dysregulation of p16 and shelterin complex.

4. Hypotheses

1. Telomere attrition and senescence in HK-2 cells were induced by oxalate, COM and KS urine, and that induction was mediated through oxidative stress.

2. Upregulation of p16 and downregulation of shelterin complex were responsible for oxidative stress-induced telomere shortening and senescence by oxalate, COM and KS urine in HK-2 cells.

5.   **Objectives**

- To investigate an induction of cellular senescence by oxalate, COM and KS urine in HK-2 cells.

- To investigate an induction of telomere shortening by oxalate, COM and KS urine in HK-2 cells.

- To investigate the oxidative stress induction by oxalate, COM and KS urine in HK-2 cells.

- To determine the expression of p16, TRF1, TRF2 and POT1 in senescent HK-2 cells induced by oxalate, COM and KS urine.

6.   **Expected benefits and applications**

In this *in vitro* experimental study, the cause-and-consequence effect of stone-associated factors (oxalate, COM and nephrolithiasis urine) on induction of oxidative stress, telomere attrition and cell senescence will be obtained. The findings of this study will contribute to the more understanding of the molecular mechanism of pathogenesis of kidney stone disease.

จุฬาลงกรณ์มหาวิทยาลัย
CHULALONGKORN UNIVERSITY

Review related literature

1. Kidney stone disease

Kidney stone is the main disease of urinary tract system which is frequently found worldwide, especially in the tropical countries (19). Studies found that prevalence of kidney stones in male and female were 12 and 6% in USA (20), 15.1 and 6.8% in Japan (21, 22), 5 and 10% in Europe (23), 4.7 and 4% in Germany (24) and 20% for both sexes in Saudi Arabia (21). In Thailand, study in 1997 showed that 16.9% of the northeastern population were attacked from this disease, (25), and our data reported in 2020 showed that the asymptomatic stone disease was found about 12% in the Northeast (26). Statistic data mentioned above show that prevalence of kidney stone disease is different among the regions. In general, stone disease is more prevalent in hot countries than in cold countries. In addition, most of studies report that stone disease is frequently found in males more than females. For example, in Germany and Iran the ratios of male-to-female are 3.13:1 and 1.15:1, respectively (27, 28). In Thailand, the male-to-female ratio is rather comparable (29, 30). Beside sex, the likelihood of kidney stone formation increases with age. Study in Japan shows that prevalence of stone disease both in men and women is more pronounced in elderly people (31). The age peak of CaOx stone is between 40 and 50 years old, whereas uric acid (UA) stone is usually found in older people (60–70 years old) (27-30). Family history is another important risk factor of stone formation. In USA, positive family history increases the risk of stone formation up to 2.57 times compared with the negative family history (32). In the Northeast of Thailand, the positive family history has approximately 3.18 times increased risk of stone formation (33). Kidney stone formation is also associated with several diseases including chronic kidney disease, end-stage renal failure, obesity, diabetes, hypertension, gout and cardiovascular

disease. Early stage of kidney stone formation is usually asymptomatic. When stone size is large enough, back pain and urinary obstruction are typical symptoms.

Mechanism of urinary stone formation remains unclear. Basically, urinary stones are classified according to stone locations including kidney or renal stone (nephrolithiasis), ureteric stone (ureterolithiasis) and bladder stone (vesical calculi) (Figure 1) (7). Most of stones are found in the kidneys, so-called kidney stone disease. The types of kidney stones are classified into four main types according to the mineral composition of stones, calcium oxalate (CaOx), calcium phosphate (CaP), magnesium ammonium phosphate (MAP) or struvite and uric acid (UA). CaOx stone is the major type of kidney stones found up to 80%. CaOx stone is often mixed with CaP stones (Hydroxyapatite). MAP or struvite stones are frequently occurred in patients with chronic urinary tract infections (urine pH>7). UA stones or urate is the second most common stone type found up to 20%. UA stone formation is associated with the low urinary pH (pH<5.05) (34). In Thailand, our study reported that the CaOx, CaP, UA and MAP stones were found at 74, 5, 16, and 5%, respectively (29).
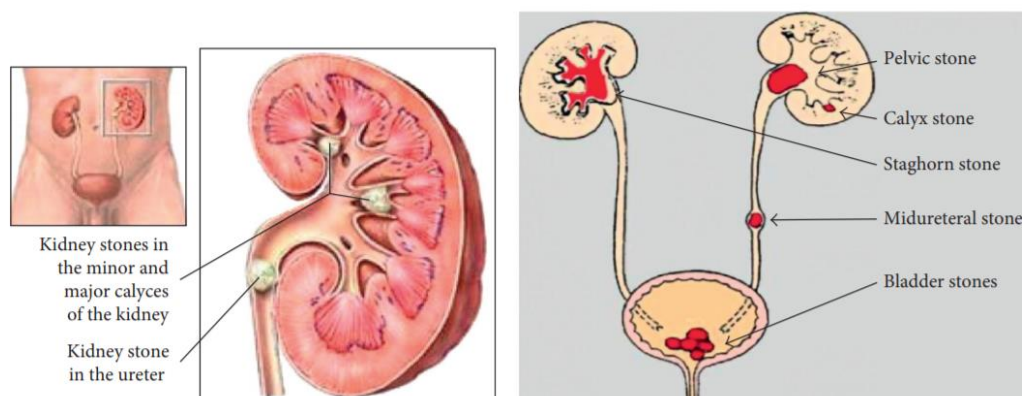
Figure 1. The locations of stone in urinary system (35).

The risk factors of stone formation involve both environmental and behavioral causes. The environmental risk factor such as loss of fluid in the hot and arid climate. The behavioral factors that are the main risk factors of stone formation such as dietary habit (36), low fluid intake, high intake of lithogenic substances (e.g., oxalate) and low

consumption of antilithogenic substances (specifically citrate). The imbalance of lithogenic and antilithogenic substances (called metabolic abnormality) leads to lithogenic crystal formation. Metabolic risk factors for stone disease include high urinary excretion of lithogenic substances such as hypercalciuria, hyperoxaluria and hyperuricosuria, and low urinary excretion of antilithogenic substances such as hypocitraturia, hypokaliuria and hypomagnesiuria. Hyperoxaluria is one of the main metabolic abnormalities for CaOx stone formation (37). Citrate is the most potent natural stone inhibitor in urine. It acts to prevent the CaOx crystallization and stone formation. Hypocitraturia is the main metabolic risk factor found in Thai stone patients. It is estimated that people with hypocitraturia have about 10-time higher risk of stone formation than those with normocitraturia (38, 39).

The initial lithogenic crystals are formed in supersaturated urine. CaOx is the most common lithogenic crystals, and the most toxic form of CaOx is calcium oxalate monohydrate (COM). There are two phases of crystal formation. One is crystal nucleation and the other is crystal growth. The nucleation is the first step of crystal formation that is induced by supersaturation of urine (40). The increased number of crystals trigger ROS production and oxidative stress in renal tubular cells leading to oxidative injury. In addition, inflammatory mediators are released from renal tubular cells after exposure to the crystals, and that leads to activation of inflammatory reaction. The injured renal tubules are the sites for the crystal adhesion. The nidus is then formed as the stone origin, and it gradually grows and finally becomes stone (Figure 2) (7).
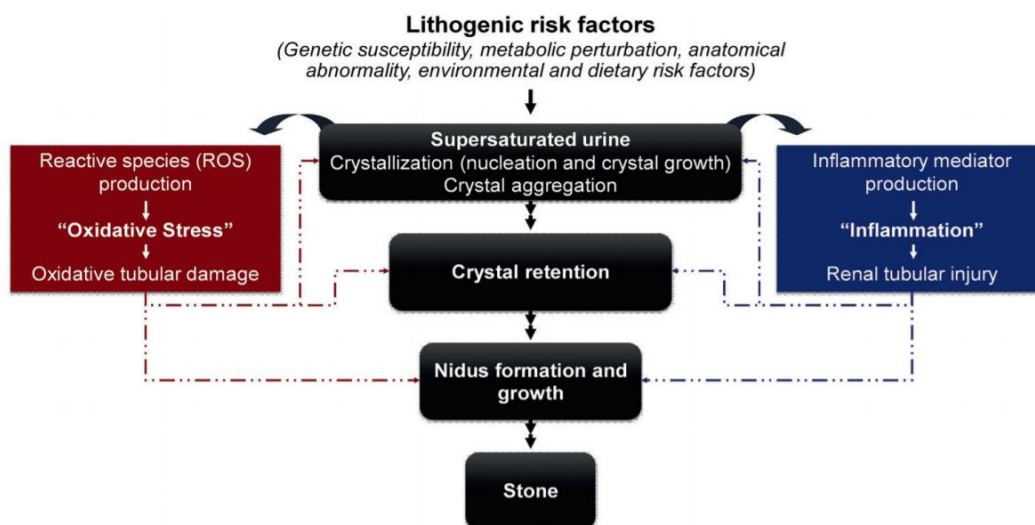
Figure 2. Schematic of the process in kidney stone formation (7).

2.   Oxidative stress

Reactive species (RS) are free radicals and non-radical reactive oxidizing agents that are chemically unstable. They are able to oxidize cellular molecules including proteins, lipids, carbohydrates and nucleotides. The main types of reactive species are reactive oxygen species (ROS) and reactive nitrogen species (RNS) (Figure 3). The common ROS is superoxide anion ($O_2•-$) that subsequently is converted to hydrogen peroxide (H_2O_2) and hydroxyl radical (•OH). RNS include nitric oxide (NO•) and peroxynitrite (ONOO-) (41). ROS are mainly generated in the electron transport system in mitochondria (42, 43). Internal factors such as metabolic process and environmental factors such as UV radiation are also the sources of ROS (44, 45). The imbalance of ROS (oxidant) production and antioxidant content results in oxidative stress that consequently causes damage of cellular molecules (46, 47). It is well-known that oxidative stress is the risk factor for the progression of many diseases such as aging-associated disease (48), atherosclerosis (49), neurodegenerative diseases (50-52) and cancers (52, 53).
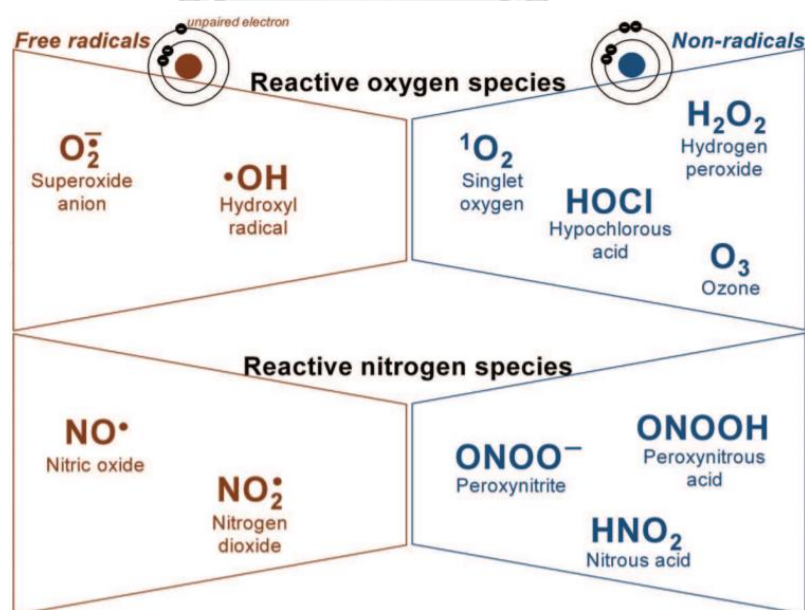
Figure 3. The main reactive species found in the human body (41).

The low concentration of ROS has physiological benefit. The superoxide anion ($O2\bullet-$) generated by NADPH oxidase is used in the respiratory burst for killing the pathogen (54). H_2O_2 is important for activation of NF-kB, the transcription factor that induces expression of genes for cellular survival, apoptosis escapade and inflammatory response (55-57). However, high generation of ROS causes oxidative damage to DNA, and the unrepaired oxidative DNA damage contributes to carcinogenesis, aging and other oxidative-mediated pathologies including nephrolithiasis (58-62).

The renal tubular cells exposed to lithogenic crystals exhibit increased production of ROS, oxidative stress, cellular injury and inflammation (63, 64). Oxidative stress and inflammation are associated with stone formation that leads to renal impairment (65, 66). In addition, oxidative stress causes DNA damage. Previous studies showed that urine and renal tubular cells of kidney stone patient contained 8-hydroxydeoxyguanosine (8-OHdG), a biomarker of oxidative DNA lesion (67, 68). 8-OHdG (8-oxo-G) is oxidatively altered from guanine (G), and G is the most sensitive base to be easily and rapidly modified by ROS (69, 70).

3.   Telomere shortening

Telomeres, the mammal chromosome ends, are associated with shelterin complex (71). Functions of shelterin is to protect the chromosome ends from DNA strand break, degradation and fusion (72). In general, the proliferation rates of human somatic cells are regulated by the length of telomere. Double-stranded (ds) telomeric chromosomes are composed of TTAGGG repeats (approximately 4-15 Kbp), called G- and C-strands (73, 74). G-strands are contained single-stranded (ss) chromosomes (approximately 100–150 nucleotides), the so-called 3' overhang (75) (Figure 4). Telomeric chromosomes are formed T- and D-loop with shelterin complex for protecting the ends of chromosome from DNA damage respond (DDR) pathway (76) (Figure 4).

Chromosome with the telomeres

Telomere TTAGGG repeat with the high guanine content and the 3' overhang

4-15 kbp   100-150 nt

TTAGGGTTAGGGTTAGGG..TTAGGGTTAGGG **3'**

AATCCCAATCCCAATCCC **5'**
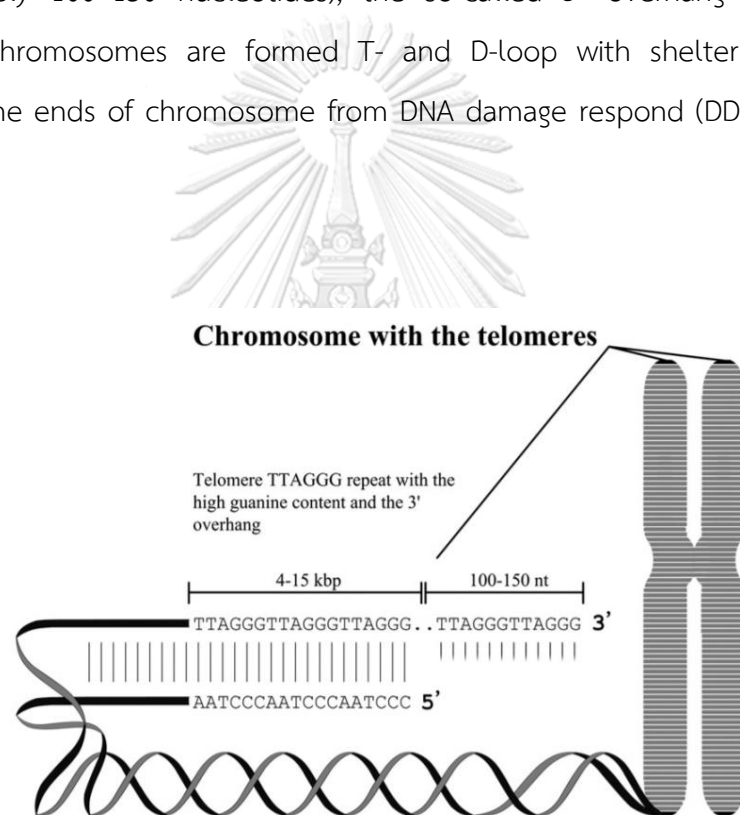
Figure 4. Structure of telomeres (77)**.**

Shelterin complex regulates the length of telomere and protects the chromosome ends. The six components of shelterin complex include telomeric repeat binding factor-1 and -2 (TRF1 and TRF2) that bind telomeric dsDNA and form t-loop structure for preventing the ends of chromosome from DNA damage mechanism and dsDNA breaks, TRF1-interacting protein-2 (TIN2) that is associated with TRF1 and TRF2

for inhibiting the elongation of telomere, protection of telomeres protein-1 (POT1) that interacts with single strand DNA and protects telomere from ssDNA breaks and DNA damage respond pathway, TIN2- and POT1-interacting protein (TPP1) that are the mediated proteins used for interaction between the six components of shelterin complex and repressor/activator protein 1 (RAP1) that binds to TRF2 for protecting chromosome from nonhomologous end-joining (78-80) (Figure 5).
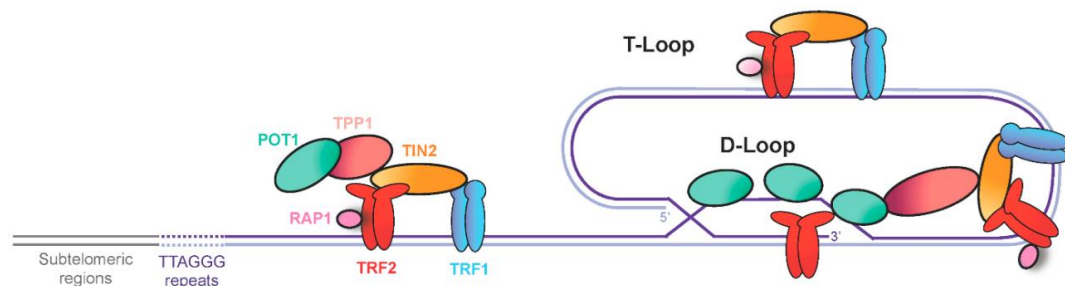
Figure 5. Telomeres with shelterin complex (81).

The telomere elongation is synthesized and maintained for unlimited replication by telomerase enzyme (82) (Figure 6). The telomerase is a complex of two parts of ribonucleoprotein including human telomerase reverse transcriptase (hTERT) that adds deoxynucleotide triphosphates at the telomeric chromosome from 5' to 3', and human RNA component (hTR) that contains template region for the reverse transcription (72, 83-85) (Figure 7). Telomerase is inactivated by hTERT inhibitor that regulates the function of telomerase (72). In general, telomerase is upregulated in the stem cells. In about 85% of cancer cells, the telomere length is maintained by the overexpression of telomerase enzyme leading to unlimited cell proliferation (86). In contrast, telomerase is downregulated or lowly expressed in somatic cells. Consequently, telomere length in somatic cells is decreased in each cycle of cell division leading to cell cycle arrest, acting as a molecular clock (87).
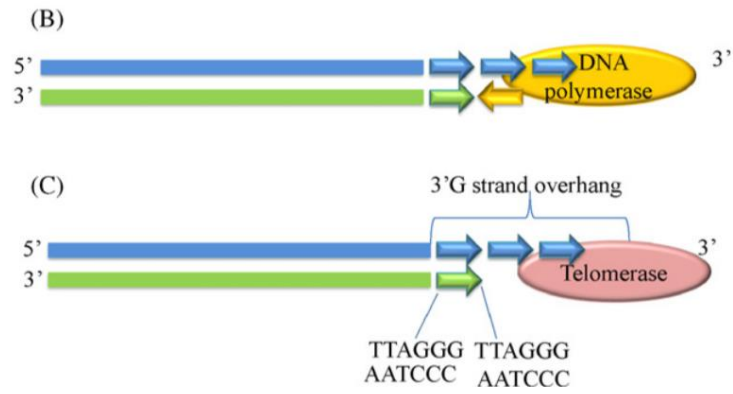
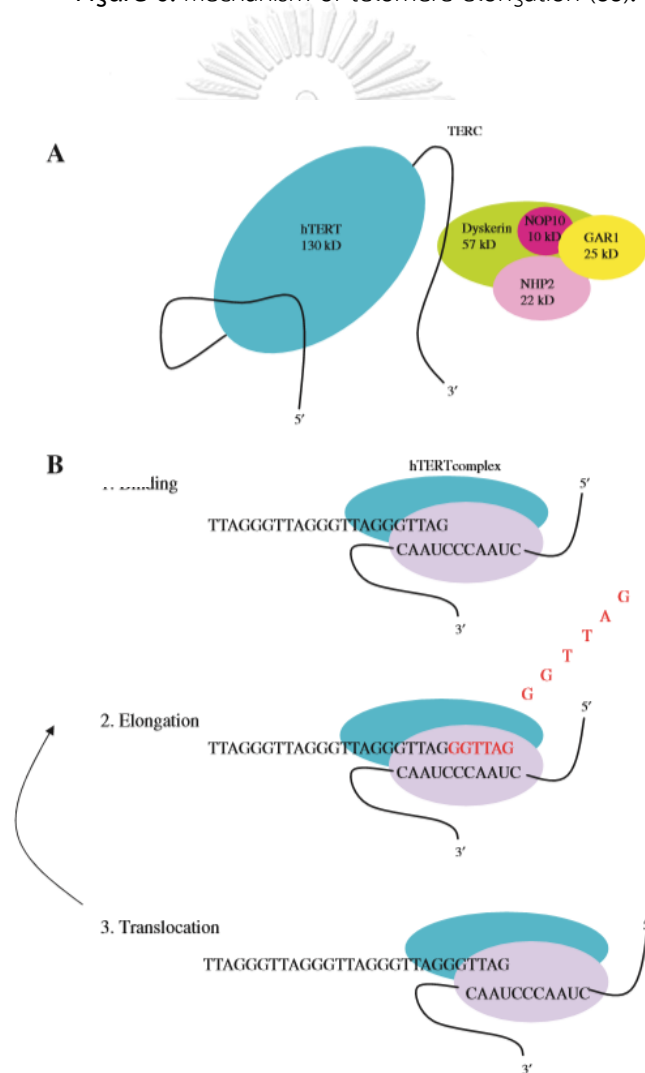**Figure 6.** Mechanism of telomere elongation (88).

Figure 7. Telomerase structure and activity (89).

In normal somatic cells, telomeres are shortened in each DNA replication (called replication problem). This is due to the fact that DNA polymerase is required a primer for replicating DNA template from 5' to 3' ends and disposed primer in lagging strand that leads to incomplete lagging strand replication and telomere shortening (90, 91). However, the internal factors affect telomere shortening rate lower than the external factors, and the external factors mainly are oxidative stress inducers (92-94).

Previous studies showed that oxidative stress accelerated telomere shortening (73). Excessive oxidative stress induces DNA base damage, single ssDNA breaks and dsDNA breaks in many locations of chromosomes. Telomere ends are susceptible to the oxidative damage because telomeres are composed of high guanine contents (95, 96). In addition, telomeric DNA depletes DNA repair mechanism compared with the non-telomeric DNA. ROS (especially H_2O_2) directly causes ssDNA breaks and interferes the oxidative base repair mechanism (97). Human fibroblasts exposed to high dose of H_2O_2 cause increased ssDNA breaks in minisatellites and telomeric DNA, and the ssDNA breaks at telomeric DNA were slowly fixed compared with the minisatellites (97). This is due to the fact that binding of TRF2 to the telomeres blocks the activity of enzyme for telomeric DNA repair, inhibits activation of ATM kinase, and interacts with polymerase β (98, 99). Accumulation of oxidative DNA lesions in the telomeres and unfixed telomeric DNA lesions leads to ssDNA breaks and telomere attrition. The consequences of critical shortening of telomeres are cellular senescence, apoptosis and carcinogenesis.

Several studies showed that telomere shortening that leads to cellular senescence is associated with development and progression of age-associated diseases, for examples, cardiovascular diseases, neurodegenerative diseases and chronic kidney diseases (CKD). In CKD, the dysfunction of telomere decreases the repairing and regeneration of kidney (100). Poor repairing and regeneration of kidney in elderly people lead to progression of CKD and end-stage kidney disease. Westhoff et

al. showed in the mice with telomerase inhibition that the kidney repairment after injury induction was much slower than the control (from 7 to 30 days) (101).

4.   Cellular senescence

Cellular senescence (aging) is the phenotype of cell cycle arrest. The senescence is the adaptive response when the body encounters the loss of homeostasis in order to reduce the risk of disease development and death. The first study to delineate the senescence mechanism was the study in human fibroblasts by Hayflick (102). Senescent cells are restrained the cell growth (cell proliferation), but their metabolic activity is remained (cell viability). They are characterized by morphological changes such as increased volume and flat cytoplasm (103). In addition, senescent cells show altered gene expression and nuclear structure. Types of cellular senescence are classified into two forms, the replicative senescence and the stress-induced premature senescence (SIPS) or aberrant signaling-induced senescence (STASIS). The main cellular markers of senescence are senescence-associated β-galactosidase (SA-βgal) and tumor suppressor protein p16^{INK4a}. These markers are increased in the senescent cells even in the absence of morphology change.

The first evidence of senescence is replicative senescence. This senescent form is directly caused by the shortening of telomeres in each cell division, and it has an important role in tumor suppression (104). When the telomeres are critically shortening, the protecting proteins are disrupted leading to activation of DDR protein p53. The activation of p53 protein leads to overexpression of p21 gene which inhibits the cyclin-dependent kinase 2 (CDK2) to activate pRb and inactivate E2F. The result of this pathway is inhibition of S-phase genes expression resulting in cellular growth arrest (G1 to S phase inhibition). Replicative senescence can be accelerated by telomere shortening via oxidative DNA damage induced by ROS (105, 106). The induction of telomere shortening by oxidative DNA damage can decrease cancer progression through replicative senescence pathway (107-112).

SIPS or STASIS is premature cellular senescence that is independent of telomere shortening or dysfunction, but it is associated with stress signals, especially ROS (113). The cytotoxic dose of cellular stress agents can induce SIPS in several cell

types including skin, lung and endothelial cells. SIPS is induced by activation of $p16^{INK4a}$, and then $p16^{INK4a}$ inhibits CDK 2/4 that further suppress phosphorylation of pRb resulting in pRb activation, inactivation of E2F, inhibition of S-phase genes expression and finally cellular growth arrest (Figure 8).
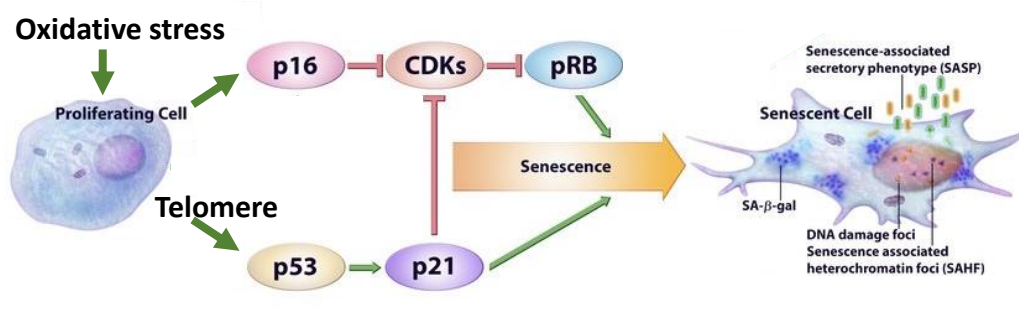
Figure 8. Cellular senescence pathway (113).

In senescent cells, the SA-βgal is the main biomarker for characterization (114). β-galactosidase enzyme in lysosome is highly activated and overexpressed in senescent cells (especially in replicative senescence). This enzyme in ageing cells is optimally detected at nearly pH 6 (17, 115, 116), but in normal cells β-galactosidase is detected at pH 4 (116). The high activity and overexpression of β-galactosidase enzyme are shown in several cell types (17, 117-119). SA-βgal is correlated with telomere shortening. For example, cellular senescence in human retinal pigment epithelial cells increases the activity and overexpression of β-galactosidase enzyme, and at the same time it decreases of telomere length from 10 kb to 4 kb (120). Increase in β-galactosidase enzyme is correlated with replicative senescence through telomere shortening.

Various studies showed that the accumulation of senescent cells was increased by age. The SA-βgal activity and $p16^{INK4a}$ expression was increased in aging individuals (114, 121, 122), and correlated with the telomere shortening in aging tissue of many cell types (122-124). Cellular senescence is associated with age-related diseases

progression including cardiovascular dysfunction, carcinogenesis, neurogenesis and the progression of acute kidney injury (Figure 9) (122-124).
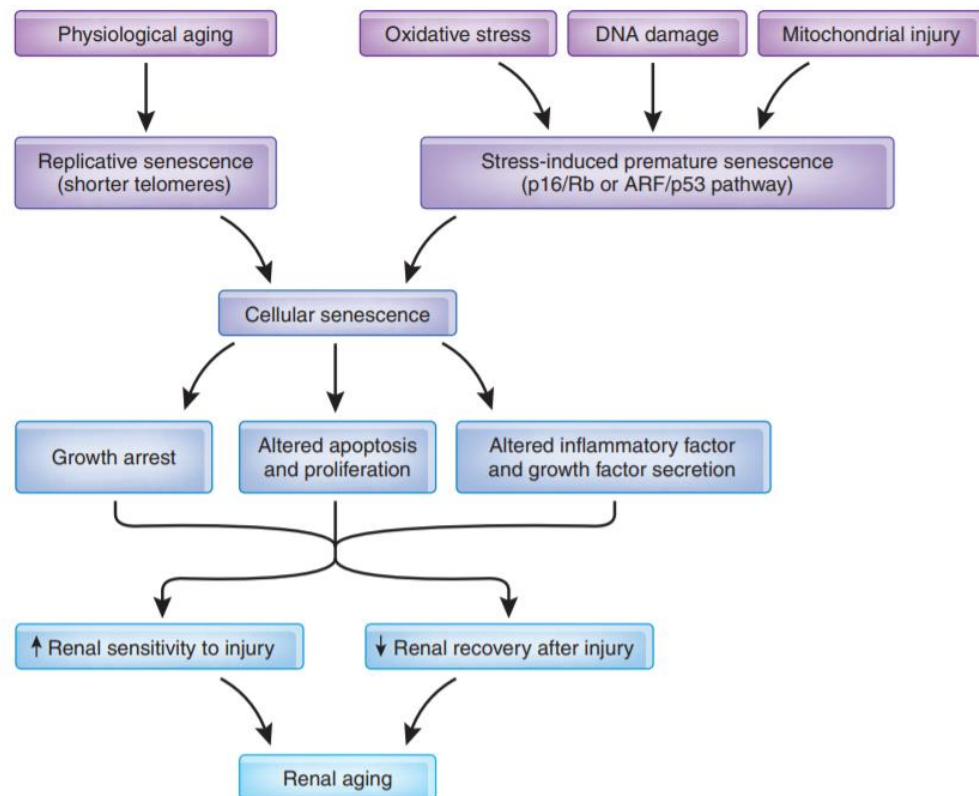
Figure 9. The diagram of renal aging (124)**.**

จุฬาลงกรณ์มหาวิทยาลัย
CHULALONGKORN UNIVERSITY

In renal senescence, the replicative senescence that associated with telomere shortening was induced by physiological aging. Furthermore, oxidative stress can accelerate renal senescence via SIPS pathway. In human and animal with renal disease, the senescence markers including SA-βgal, and p16^{INK4A} were detected (125-127). The accumulation of renal senescent cells leading to proliferation imbalance, changing the inflammatory and growth factor, increases in renal injury, decreases in renal repairing after injury and renal aging (Figure 9) (122-124). The characteristics of renal senescence is the loss of renal mass which is mainly found in proximal tubular cells (PTC) of renal cortex compared with the medulla. This leads to renal fibrosis decreased GFR. This

process is usually accelerated in elderly (50 to 60 years old) (128-130). Increased vascular resistance and decreased renal blood flow are also observed (131).

The maintenance of telomere length and inhibition of p16^{INK4a} expression are the mainly treatment method of age-related renal disease. Telomere length is maintained by telomerase, but telomerase is the oncogenic gene. The upregulation of shelterin complex is another way for preventing the damage of telomeric ends (132). Since the telomere shortening is accelerated by oxidative stress, antioxidant intervention is another option for preventing renal senescence (133). In general, approaches to decrease oxidative stress and increase antioxidant capacity (including exercises) are suggested for reducing the accumulation of senescent cells, and hence reducing the risk of renal disease development and progression.

Conceptual framework

Kidney stone disease predisposition increases with age.
Kidney stone patients have increased oxidative stress compared with non-stone subjects. Premature senescence is known to be induced by oxidative stress. High urinary oxalate, and increased CaOx crystallization are the main risk factors of CaOx nephrolithiasis.

We hypothesized that oxalate, COM and urine from kidney stone patient induced telomere shortening and premature senescence in renal tubular cells through

Oxalate (NaOx)   COM   Urine ↑ Ox

Normal cell (HK-2 cells)

Proliferating Cell

↑ ROS
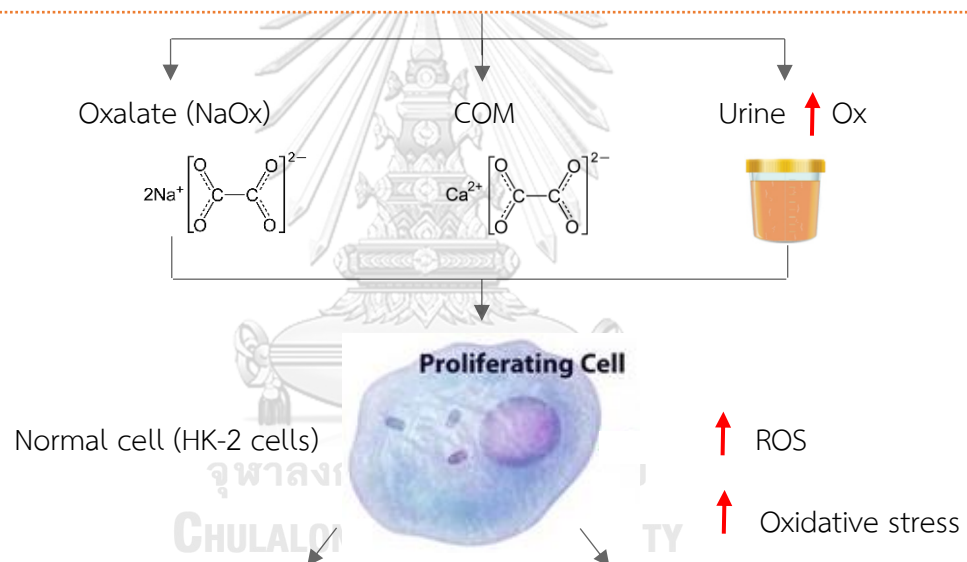
↑ Oxidative stress

- Low expression of Shelterin proteins (TRF1, TRF2 and POT1)
- Increased oxidative DNA damage

↑ p16

↑ Telomere attrition

Cellular senescence

Experimental design

This research was an *in vitro* study investigated in cell culture model. Telomere shortening and senescence in HK-2 cells induced by oxalate, COM, kidney stone (KS) and non-stone (NS) urine were determined. Hydrogen peroxide, a known factor for inducing oxidative stress, cellular senescence and telomere shortening, was served as positive control in this study. Levels of oxalate in urine were measured by oxalate oxidase. Capability of urine to crystallize CaOx was determined by iCOCI and COCI assay. KS urine (n=5) that was used in the experiments had significantly higher levels of urinary oxalate, iCOCI and COCI than the age- and sex-matched NS urine (n=5). In cell culture experiments, treatment conditions were divided into 14 groups including, untreated control, H_2O_2, NaOx, COM, 5 for KS urine and 5 for NS urine as shown below.
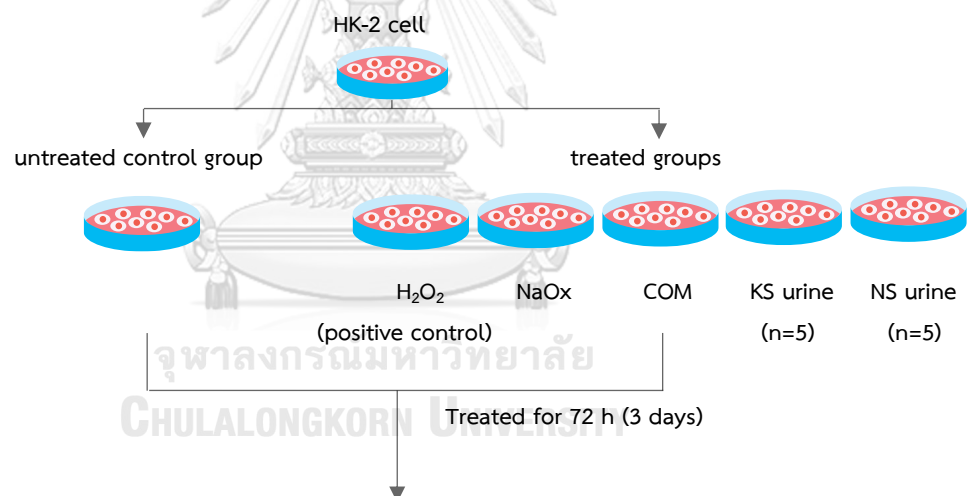
Cytotoxicity
- Cell viability (MTT assay)

Oxidative stress
- Protein carbonylation (DNPH assay)
- Total antioxidant capacity (TAC) (ABTS assay)

Cellular senescence
- SA-βgal staining
- p16 (Immunocytofluorescent staining and western blot)

Telomere shortening
- Relative telomere length (Real-time qPCR)
- TRF1, TRF2 and POT1 gene expression (Real-time qPCR)

Research methodology

1.   Materials and chemicals

Equipment and chemicals used in this study were listed in Table 1 and Table 2, respectively.

Table 1. List of equipment used in this study

Materials	Companies
Autoclave	Hirayama, Saitama, Japan
Autopipette 10, 100, 1000 μL	Bio-rad, California, USA
Cell culture dish 25, 50, 75 cm^2	Corning, New York, USA
Cell culture plates 6-, 96-well	Corning, New York, USA
ChemiDoc MP Imaging System	Bio-rad, California, USA
Class II biohazard safety cabinet	Esco Technologies, Pensylvania, USA
CO_2 Incubator	Thermo Scientific, Ohio, USA
Cryotube	SPL lifescience, Gyeonggi-do, South Korea
Cuvettes (Plastic)	Perkin Elmer, USA
Distilled water maker	Thermo Scientific, Ohio, USA
Freezer (-20, -80°C)	Sanyo Electric, Osaka, Japan
Horizontal electrophoresis system	Bio-rad, California, USA
Invitrogen™ EVOS™ FL Auto 2 Imaging System	Thermo Scientific, Ohio, USA
Microcentrifuge tubes	Axygen, California, USA
Microplate reader	Thermo Scientific, Ohio, USA
NanoDrop™ 2000/2000c Spectrophotometers	Thermo Scientific, Ohio, USA
QuantStudio™ 5 Real-Time PCR System	Thermo Scientific, Ohio, USA
Sterile pipette 10 mL	Corning, New York, USA
Syringe filter nylon 0.22 μm.	Ageia Technologies, USA
Votex mixer	Vortex-2 Genie, USA
Water bath	GFL, Burgwedel, Germany

Table 2. Chemicals used in this study

Chemicals	Companies
2,2′-Azino-bis (3-ethylbenzothiazoline-6-sulfonic acid) (ABTS)	Sigma-Aldrich, Missouri, USA
2,2′-Azobis(2-methylpropionamidine) dihydrochloride (AAPH)	Sigma-Aldrich, Missouri, USA
2,4-Dinitrophenylhydrazine (DNPH)	TCI America, Tokyo, Japan
3-(4,5-dimethylthiazol-2-yl)-2,5-diphenyl tetrazolium bromide (MTT)	Sigma-Aldrich, Missouri, USA
4′,6-Diamidino-2-phenylindole dihydrochloride	Sigma-Aldrich, Missouri, USA
5-Bromo-4-Chloro-3-Indolyl β-D-Galactopyranoside (X-gal)	Vivantis, Buckinghamshire, Malaysia
Alexa Fluor® 488 Goat Anti-Rabbit (IgG)	Cell Signaling Technology Danvers, MA, USA
Anti-CDKN2A/p16INK4a antibody	Abcam, Cambridge, UK
Anti-rabbit IgG, HRP-linked antibody	Cell Signaling Technology Danvers, MA, USA
Calcium oxalate monohydrate	Merck Millipore, Massachusetts, USA
Citric acid	Merck Millipore, Massachusetts, USA
Dulbecco's modified eagle medium (DMEM)	Hyclone, Logan UT, USA
ECL Western Blotting Substrate	Thermo Scientific, Ohio, USA
Ethanol	Merck Millipore, Massachusetts, USA
Ethyl acetate	Merck Millipore, Massachusetts, USA
Fetal bovine serum (FBS)	Hyclone, Logan UT, USA
Fluoroshield mounting medium with DAPI	Abcam, Cambridge, UK
37% Formaldehyde	Merck Millipore, Massachusetts, USA
GF-1 Tissue DNA Extraction Kit	Vivantis, Buckinghamshire, Malaysia
GF-1 Total RNA Extraction Kit	Vivantis, Buckinghamshire, Malaysia
Glutaraldehyde	Merck Millipore, Massachusetts, USA
Green PCR Master Mix Direct-Load, 2×	Biotechrabbit, Berlin, Germany
Guanidine hydrochloride (GdmCl)	Sigma-Aldrich, Missouri, USA
Halt™ Protease Inhibitor Cocktail	Thermo Scientific, Ohio, USA
Hydrochloric acid (HCl)	Merck Millipore, Massachusetts, USA
Loading dye	Thermo Scientific, Ohio, USA

Chemicals	Companies
Magnesium chloride (MgCl$_2$)	Merck Millipore, Massachusetts, USA
N, N-Dimethylformamide	Merck Millipore, Massachusetts, USA
Normal horse serum	Gibco, California, UK
Paraformaldehyde	Merck Millipore, Massachusetts, USA
Penicillin-streptomycin	Gibco, California, UK
Pierce™ BCA Protein Assay Kit	Thermo Scientific, Ohio, USA
Polyvinylidene difluoride (PVDF) membrane	Merck Millipore, Massachusetts, USA
Potassium ferrocyanide K$_4$[Fe(CN)$_6$]	Merck Millipore, Massachusetts, USA
Potassium hexacyanoferrate (III) K$_3$[Fe(CN)$_6$]	Merck Millipore, Massachusetts, USA
Skin milk	Sigma-Aldrich, Missouri, USA
Sodium chloride	Merck Millipore, Massachusetts, USA
Sodium oxalate	Sigma-Aldrich, Missouri, USA
Trypsin/EDTA	Gibco, California, UK
TaqMan™ Reverse Transcription kit	Thermo Scientific, Ohio, USA
Trichloroacetic acid (TCA)	Merck Millipore, Massachusetts, USA
Triton X-100	Amresco, US

2. Studied population and urine specimens

In this study, the used human urine specimens were from our previous project, entitled "Test accuracy of urinary calcium oxalate crystallization index (COCI) for diagnosis of urolithiasis and development of an innovative quantum dot nanoparticle-based method for determination of urinary oxalate (IRB: 286/59)". The urine specimens were 24-h urine specimens collected from KS patients and NS volunteers who lived in Mahasarakham province between 2017 and 2018. The inclusion and exclusion criteria for recruiting NS forming control group included 18 years old and above, both males and females, no urinary tract infection and no KS history. In the KS group, the inclusion and exclusion criteria were aged 18 years old and above, admitted for treatment at

Mahasarakham Hospital, and no malignant conditions. A total of 281 subjects were recruited divided into 129 NS subjects and 152 KS patients. Urine specimens (n=5 for each group) that used in this study were selected from these mentioned 24-h urine specimens, based mainly on urinary oxalate, iCOCI and COCI levels.

3.   Cell culture

The HK-2 cells were used in this study. The cells were maintained in DMEM (Hyclone, Logan UT, USA) with 10% FBS (Hyclone, Logan UT, USA) and 1% penicillin-streptomycin (Gibco, California, UK) at 37 °C in 5% CO_2 incubator. Cells were grow until reaching about 70-80% confluence, then sub-culturing (trypsinization) with Trypsin/EDTA (Gibco, California, UK) was performed. The 14 treatment conditions performed in this study included untreated control, H_2O_2, NaOx, COM, 5 different KS urine samples and 5 different NS urine samples. The treatment period was 72 h (3 days) in order to successfully induce the senescent phenotype. All cells were used in the experiments that were cells in the passages between 65th and 67th.

จุฬาลงกรณ์มหาวิทยาลัย
CHULALONGKORN UNIVERSITY

4.   **Cell viability**

Cytotoxicity of each stress inducer was tested using MTT assay. HK-2 cells were treated with various concentrations of H_2O_2, NaOx, COM, KS urine and NS urine for 72 h. Then, the cells were incubated with 0.5 mg/mL MTT reagent (Sigma-Aldrich, Missouri, USA) at 37 °C in 5% CO_2 incubator for 2 h. The viable cells that contained the mitochondrial oxidoreductase enzyme reduced the MTT reagent (yellow) into formazan crystals (purple).

For morphology investigation, the viable cells were washed twice with PBS and nuclei were labeled by DAPI (Sigma-Aldrich, Missouri, USA). The viable cells and nuclei were visualized under the light and fluorescence microscopes, respectively.

For quantitative absorbance measurement, the formazan crystals were dissolved in dimethyl sulfoxide (DMSO). The absorbance was measured at 570 nm by a microplate reader (Thermo Scientific, Ohio, USA). Finally, the percent of cell viability was calculated using the formula shown below.

% of cell viability = (OD of each condition/OD of control condition) x 100
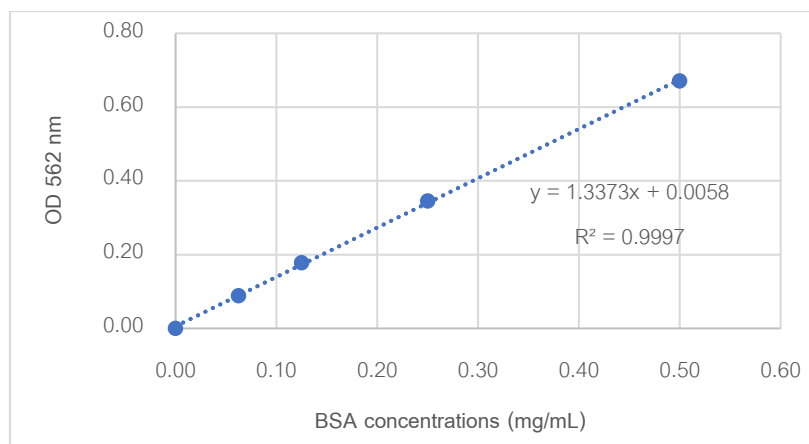
5. **Measurement of oxidative stress markers**

5.1 **Protein extraction**

After 3-day treatment, HK-2 cells were washed with PBS twice. 5 mL of RIPA buffer containing 50 µL Halt™ Protease Inhibitor Cocktail (Thermo Scientific, Ohio, USA) was added and incubated at 4 °C for 15 min. Then, the cells were harvested by cell scraper and transferred into new microcentrifuge tubes. After that, the cells were incubated at 4 °C for 30 min (vortexing every 10 min). Finally, the lysate was centrifuged at 10,000 x g at 4 °C for 15 min, and the supernatant was collected and kept at -20 °C for further testing.

5.2 **Protein concentration determination**

Protein concentration in cell lysate was determined by BCA assay. Pierce™ BCA Protein Assay Kit (Thermo Scientific, Ohio, USA) was prepared using mixing 196 µL reagent A with 4 µL reagent B. Next, 25 µL of extracted protein or various concentrations of standard bovine serum albumin (BSA) form Pierce™ BCA Protein Assay Kit was added to 200 µL BCA reagent and incubated at 37 °C for 30 min in dark. Protein was reacted with the BCA reagent, and the color turned from green to purple. The absorbance at 562 nm was measured using a microplate reader (Thermo Scientific, Ohio, USA). The protein concentrations in cell lysate sample were calculated from the BSA concentrations standard curve (Figure 10).

Figure 10. The standard curve of various concentrations of BSA

5.3 Measurement of protein carbonylation by DNPH assay

Protein carbonyl content is a maker of protein oxidation under oxidative stress. It was formed by oxidative modification of the amino acid side chains. These carbonyl groups on protein were determined using DNPH assay. Briefly, 62.5 µL of extracted protein was incubated with 250 µL of 10 mM DNPH (TCI America, Tokyo, Japan) and 250 µL of 2 N HCl (blank) at room temperature for 1 h in dark. Then, the reaction was added with 300 µL of 20% TCA (Merck Millipore, Massachusetts, USA), mixed by vortexing, incubated at 4 °C for 10 min and centrifuged at 10,000 x g at 4 °C for 15 min. The pellet was collected, added with 625 µL of 1 Ethanol:1 Ethyl acetate (Merck Millipore, Massachusetts, USA), mixed and centrifuged at 10,000 x g at 4 °C for 20 min. The pellet was added with 300 µL of 6 M GdmCl (Sigma-Aldrich, Missouri, USA), mixed by vortexing, and incubated in a heat box at 60 °C for 30 min. The absorbance was measured at 375 nm. The formula shown below was used for calculating the protein carbonyl level.

$$\text{Protein carbonyl content (nmol/mg protein)} = \frac{\text{Absorbance 375 x 45.45 (nmol/L)}}{\text{Total protein concentratin (mg/mL)}}$$

5.4 Measurement of total antioxidant capacity (TAC) by ABTS assay

The TAC was measured by ABTS assay. Briefly, 2.5 mM ABTS reagent (Sigma-Aldrich, Missouri, USA) was converted to blue/green $ABTS^+$ radical solution by reacting with 1 mM AAPH reagent (Merck Millipore, Massachusetts, USA) in PBS. The mixture was incubated at 68 °C for 40 min for converting ABTS into $ABTS^+$ radicals. Then, the blue/green $ABTS^+$ radical solution was diluted with PBS until achieving the absorbance of 0.650 ± 0.02 at 734 nm. For the reaction, 5 µL extracted protein was added into 295 µL $ABTS^+$ radical solution and incubated at 37 °C for 10 min in the dark. The $ABTS^+$ radical solution (blue/green) was reduced by the antioxidants in the testing sample. The color was changed from blue/green to colorless proportionated to amounts of antioxidants. The absorbance at 734 nm was measured. The ABTS reaction of various concentrations of vitamin C standards were performed to be used for generating the standard curve (Figure 11). Percent antioxidant activity (%AA) was calculated according to the formula shown below. TAC of the sample was calculated from the standard curve of %AA and vitamin C concentrations. Level of TAC in sample was expressed as vitamin C equivalent antioxidant capacity (VCEAC) either in the vitamin C units of mM or mg/L.
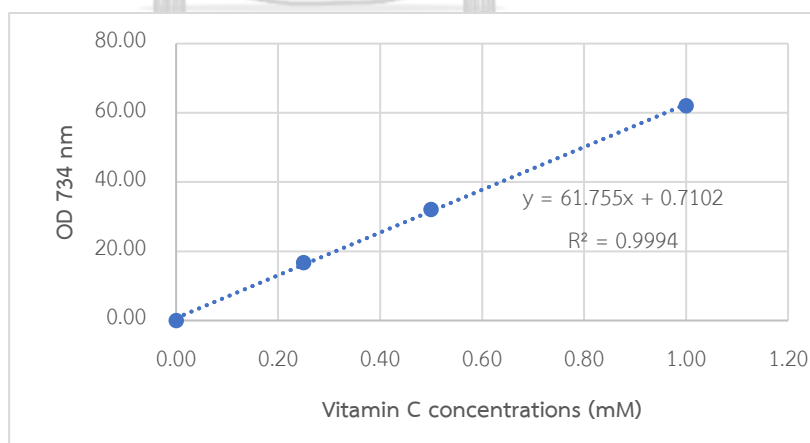
Figure 11. The standard curve of various concentrations of vitamin C

$$\% \text{ Antioxidant activity (\%AA)} = \frac{(\text{OD Blank} - \text{OD sample})}{\text{OD Blank}} \times 100$$

TAC (VCEAC, mg/L) = VCEAC (mM) x 176.12 (molecular weight of vitamin C)

6.   Cellular senescence detection

6.1   SA-βgal staining

The best characterized marker of senescence is the lysosomal β-galactosidase enzyme, so-called SA-βgal. In normal cell, the optimal pH of this enzyme is at pH 4, but in senescent cells it is optimally working at pH 6. The staining solution was prepared by mixing of 40 µL of 50 mg/mL X-gal solution (Vivantis, Buckinghamshire, Malaysia) in N, N-Dimethylformamide (Merck Millipore, Massachusetts, USA), 1.74 mL of 0.2 M citric acid/sodium phosphate buffer (pH=6) (Merck Millipore, Massachusetts, USA), 50 µL each of 200 mM potassium hexacyanoferrate and potassium ferrocyanide (Merck Millipore, Massachusetts, USA), 100 µL 5 M NaCl (Merck Millipore, Massachusetts, USA) and 20 µL 5 M $MgCl_2$ (Merck Millipore, Massachusetts, USA). Of note, this solution must be freshly prepared. Before staining, the cells were fixed with 37% formaldehyde and 50% glutaraldehyde (Merck Millipore, Massachusetts, USA) in PBS for 5 min. After washing twice with PBS, cells were stained with the staining solution at 37 °C for 12-16 h. The staining cells were washed with PBS two time and senescent cells were labeled in blue under the light microscope.

6.2   Immunocytofluorescent staining of p16

The p16 protein is the best-known marker of SIPS induced by oxidative stress. In this study, p16 was detected by immunofluorescent staining. Briefly, the cells (on coverslip) were fixed with 4% paraformaldehyde (Merck Millipore, Massachusetts, USA) for 10 min, incubated in 0.1% Triton X-100 (Amresco, US) for 3 min (permeabilization) and washed twice with PBS. Next, the fixed cells were blocked for the non-specific binding by 1% normal horse serum (Gibco,

California, UK) in PBS at 37 °C for 1 h. After that, the primary antibody p16 antibody (1:10,000) (Abcam, Cambridge, UK) was added into the cells and incubated at 4 °C overnight. Then, the cells were washed with PBS and incubated with secondary antibody Alexa Fluor® 488 Goat Anti-Rabbit (IgG) (1:10,000) (Cell Signaling Technology Danvers, MA, USA) in PBS at 37 °C for 30 min in dark. Finally, the slides were mounted with fluoroshield mounting medium with DAPI (Abcam, Cambridge, UK). p16-positive cells were visualized under the fluorescence microscope.

6.3   Western blot of p16 protein

Western blot with immunodetection is the common detection of specific protein using gel electrophoresis. Briefly, 5% stacking gel and 12% separating gel were prepared, and 10 µg extracted protein with 3 µL loading dye (Thermo Scientific, Ohio, USA) were incubated at 95 °C for 5 min. The gel electrophoresis was set at 100 V for 20 min and the voltage was then increased to 200 Volt for 1 hr. Then, protein was transferred to PVDF membrane (Merck Millipore, Massachusetts, USA), and the membrane was incubated with 5% skin milk (Sigma-Aldrich, Missouri, USA) in TBS-T for 1 h. Then, it was incubated with primary antibody p16 (1:10,000) (Abcam, Cambridge, UK) and GAPDH (1:10,000) (Cell Signaling Technology Danvers, MA, USA) at 4 °C overnight. Then, the membrane was washed twice with TBS-T and incubated membrane with secondary anti-rabbit IgG, HRP-linked antibody (1:10,000) (Cell Signaling Technology Danvers, MA, USA). p16 and GAPDH immunocomplexes were detected using ECL Western Blotting Substrate (Thermo Scientific, Ohio, USA) and imaged by the ChemiDoc MP Imaging System (Bio-rad, California, USA). The relative density of p16 and GAPDH protein bands was measured using Bio-Rad's New Image Lab™ Software (Bio-rad, California, USA)

7. Telomere shortening

7.1 DNA extraction and concentration

The genomic DNA was extracted from the treated HK-2 cells using GF-1 Tissue DNA Extraction Kit (Vivantis, Buckinghamshire, Malaysia), performed according to the manufacturer's instructions. Briefly, the cell pellet was resuspended with 200 µL of PBS, added with 20 µL of proteinase K, 2 µL of lysis enhancer and 200 µL of buffer TB, mixed well by pulsed-vortexing and then incubated at 65 ℃ for 10 min. After that, the lysate was added with 200 µL of absolute ethanol and mixed immediately by pulsed-vortexing. The mixture of 650 µL was transferred into the column from extraction kit, centrifuged at 5,000 x g for 1 min and discarded flow through. The column was washed by 650 µL washing buffer, centrifuged at 5,000 x g for 1 min, discarded flow through and washed once again. The column was centrifuged at 10,000 x g for 1 min to remove all traces of ethanol. The column was placed into the new microcentrifuge tube. 75 µL of elution buffer (preheated at 65 ℃) was added, incubated at room temperature for 3 min and centrifuged at 5,000 x g for 1 min to elute DNA. The concentration of DNA was measured based on absorbance at 260 and 280 nm by NanoDrop™ 2000/2000c Spectrophotometers. The ratio of 260/280 nm between 1.8 and 2.0 indicates the high-quality of DNA. DNA was stored at -20 ℃ for qPCR experiment.

7.2   Determination of relative telomere length (RTL) by real-time qPCR

The RTL was determined by the real-time qPCR with SYBR green format. Briefly, the DNA and the primers specific for telomeres and 36B4 gene (Table 3) were diluted to 1.56 ng/µL and 10 µM, respectively, with distilled water. For the qPCR reaction, the 8 µL of master mix (Biotechrabbit, Berlin, Germany) and 2 µL of diluted DNA or distilled water (for negative control) were added into the PCR tubes (Table 4). The condition of real-time qPCR was shown in Table 5. The Ct values obtained from the real-time qPCR were used for calculation of the relative telomere length according to the formula shown below.

$$\Delta Ct_{ref} = Ct\ Tel_{ref} - Ct\ 36B4_{ref}$$

$$\Delta Ct_{sam} = Ct\ Tel_{sam} - Ct\ 36B4_{sam}$$

$$\Delta\Delta Ct = \Delta Ct_{sam} - \Delta Ct_{ref}$$

$$\text{Relative telomere length} = 2^{-\Delta\Delta Ct}$$

Ct: cycle threshold

ref: control

sam: H_2O_2, NaOx, COM, KS and NS urine

Table 3. The primer sequences for telomere length measurement (134).

Primer's name	Sequence
Telomere (Forward)	5'-CGGTTTGTTTGGGTTTGGGTTTGGGTTTG GGTTTGGGTT-3'
Telomere (Reverse)	5'-GGCTTGCCTTACCCTTACCCTTACCCTTACCC TTACCCT-3'
36B4 (Forward)	5'-CAGCAAGTGGGAAGGTGTAATCC-3'
36B4 (Reverse)	5'-CCCATTCTATCATCAACGGGTACAA-3'

Table 4. The master mix for telomere length measurement (134).

Chemical reagent	Volume (µL)
SYBR master mix (2x)	5
Forward primers (10 µM)	0.2
Reverse primers (10 µM)	0.2
Distilled water	2.6
total	8

Table 5. The real-time qPCR condition for telomere length measurement (134).

PCR cycle	Temperature (℃)	Time (minutes)	cycle
Holding stage	95	10.00	1
Denature	95	0.15	40
Annealing	54	1.00	

7.3   RNA extraction and concentration measurement

The RNA was extracted from HK-2 cells by GF-1 Total RNA Extraction Kit (Vivantis, Buckinghamshire, Malaysia), performed according to manufacturer's instructions. Briefly, the cells were added with 350 µL of buffer TR and mixed well by pulsed-vortexing. The lysate was further transferred into the homogenization column, centrifuged at maximum speed for 2 min and collected the flow through. The column was added with 350 µL of 80% ethanol to the flow through and mixed thoroughly by pipetting. The 650 µL of sample including any precipitate was transferred into RNA binding column, centrifuged at 10,000 x g for 1 min and discarded flow through. The column was washed with 500 µL washing buffer, centrifuged at maximum speed for 1 min and discarded the flow through. The column was added with 70 µL of DNase I digestion Mix and incubated at room temperature for 15 min. The column was

added with 500 µL of inhibitor removal buffer, centrifuged at maximum speed for 1 min, discarded flow through and washed once again with washing buffer. The column was centrifuged at 10,000 x g for 1 min to remove all traces of buffer. The column was placed into the new microcentrifuge tube, added 30 µL of RNase-free water directly onto the membrane, incubated at room temperature for 1 min and centrifuged at 10,000 x g for 1 min to elute the RNA. The concentration of RNA was measured by absorbance at 260 and 280 nm by NanoDrop™ 2000/2000c Spectrophotometers. The ratio of 260/280 nm between 1.8 and 2.0 indicate the high-quality of RNA. RNA was stored at -20 °C for complementary DNA (cDNA) reversion.

7.4   cDNA reverse transcription

The cDNA was conversed using TaqMan™ Reverse Transcription kit (Thermo Scientific, Ohio, USA). Briefly, 1 µL of 10 µg RNA template and 2.5 µM Oligo d(T)16 was added into the PCR tubes, and incubated template RNA and primers at 65 °C and 5 °C for 5 and 2 min, respectively. After that, 18 µL of RT master mix was added to template RNA and primers (Table 6) and incubated at 37 °C for 30 min and 95 °C for 5 min, and held at 4 °C. Converted cDNA was stored at -20 °C for qPCR experiment.

<p align="center">Table 6. The RT master mix for cDNA reverse transcription.</p>

Chemical reagent	Volume (µL)
10x RT buffer	2.0
25 mM MgCl$_2$	1.4
10 mM dNTP mix	4.0
RNaes Inhibitor (20 U/ µL)	1.0
MultiScribe™ Reverse Transcriptase (50 U/ µL)	1.0
DEPC-treated water	8.6
total	18

7.5 TRF1, TRF2 and POT1 gene expression (real-time qPCR)

TRF1, TRF2 and POT1 mRNA expression were determined by reverse transcription-qPCR. The primers specific for TRF1, TRF2, POT1 and GAPDH genes are shown in Table 7. The primers were diluted to 10 µM with distilled water. The 8 µL master mix (Biotechrabbit, Berlin, Germany) (Table 8) and 2 µL of cDNA or distilled water (for negative control) were placed into the PCR microcentrifuge tubes. The condition of real-time PCR is shown in Table 9. The Ct value obtained from the real-time qPCR was used for calculation of the relative mRNA expression according to the formula shown below.

$$\Delta Ct_{ref} = Ct\ Sel_{ref} - Ct\ GAPDH_{ref}$$
$$\Delta Ct_{sam} = Ct\ Sel_{sam} - Ct\ GAPDH_{sam}$$
$$\Delta\Delta Ct = \Delta Ct_{sam} - \Delta Ct\ GAPDH_{ref}$$
$$Ratio = 2^{-\Delta\Delta Ct}$$

Ct:	cycle threshold
Sel:	TRF1, TRF2 and POT1
ref:	control
sam:	H$_2$O$_2$, NaOx, COM, KS and NS urine

Table 7. The primer sequences for gene expression analysis (135).

Primer's name	Sequence
TRF1 (Forward)	5'- GCTGTTTGTATGGAAAATGGC -3'
TRF1 (Reverse)	5'- CCGCTGCCTTCATTAGAAAG -3'
TRF2 (Forward)	5'- GACCTTCCAGCAGAAGATGCT -3'
TRF2 (Reverse)	5'- GTTGGAGGATTCCGTAGCTG -3'
POT1 (Forward)	5'- TCAGATGTTATCTGTCAATCAGAACCT -3'
POT1 (Reverse)	5'- TGTTGACATCTTTCTACCTCGTATAATGA -3'
GAPDH (Forward)	5'- AACGTGTCAGTGGTGGACCTG -3'
GAPDH (Reverse)	5'- AGTGGGTGTCGCTGTTGAAGT -3'

Table 8. The master mix for gene expression analysis (135).

Chemical reagent	Volume (µL)
SYBR master mix (2x)	5
Forward primers (10 µM)	0.2
Reverse primers (10 µM)	0.2
Distilled water	2.6
total	**8**

Table 9. The real-time qPCR condition for gene expression analysis (135).

PCR cycle	Temperature (℃)	Time (minutes)	cycle
Holding stage	95	10.00	1
Denature	95	0.15	
Annealing	60	0.20	40
Extension			

8. **Statistical analysis**

The data were presented in mean ± standard deviation (SD). The categorical variables were presented as frequency and percent. T-test was used to test the difference between two groups of numeric data. All of statistics and graphs in this study were calculated by the GraphPad Prism Software version 8.0 (GraphPad Software, San Diego, CA). $P<0.05$ was considered statistically significant.

จุฬาลงกรณ์มหาวิทยาลัย
CHULALONGKORN UNIVERSITY

Results

1.   Characteristics of 24-h urine specimens treated in HK-2 cells

In this study, a total of 10 24-h urine specimens obtained from 5 KS patients and 5 age- and sex- matched NS individuals were used for treating with HK-2 cells. Age (57.600 ± 6.229 vs. 58.400 ± 6.877 years), BMI (22.974 ± 33.111 vs. 22.213 ± 3.410 kg/m^2), 24-h urine volume (1862.000 ± 1401.274 vs. 1676.000 ± 403.150 mL) and urine creatinine (2.102 ± 0.490 vs. 1.767 ± 2.105 g/day) of the selected NS and KS subjects were not significantly different (Table 10). In contrast, urinary levels of oxalate (18.584 ± 14.313 vs. 4.017 ± 1.303 mg/day), iCOCI (3.817 ± 1.732 vs. 0.140 ± 0.169 COM equiv. g/day) and COCI (1.860 ± 1.092 vs. 0.403 ± 0.266 COM equiv. g/day) in KS subjects were significantly higher than that in the NS subjects (Table 10).

จุฬาลงกรณ์มหาวิทยาลัย

CHULALONGKORN UNIVERSITY

Table 10. The characteristics of 24-h urine specimens used in the study.

	Age (years)	Sex	BMI (kg/m^2)	24-h urine vol. (mL)	Urine Cr (g/day)	Urine Ox (mg/day)	Urine iCOCI (COM equiv.g/day)	Urine COCI (COM equiv.g/day)
Non-stone case (NS)								
NS#002	62	female	21.453	780	1.920	1.980	0.070	0.443
NS#124	64	male	19.531	2310	2.896	4.325	0.108	0.220
NS#200	56	male	24.167	1000	1.689	5.499	0.081	0.173
NS#204	48	male	22.032	1090	2.233	4.539	0.006	0.337
NS#195	58	male	27.689	4130	1.771	3.742	0.435	0.840
Avg. (mean ± SD)	57.600 ± 6.229	-	22.974 ± 33.111	1862.000 ± 1401.274	2.102 ± 0.490	4.017 ± 1.303	0.140 ± 0.169	0.403 ± 0.266
CaOx-stone case (KS)								
KS#258	66	female	26.639	1360	0.120	31.655	4.820	3.350
KS#249	64	male	19.228	1350	0.196	13.320	2.882	1.859
KS#233	53	male	18.377	1850	2.298	35.598	6.060	2.458
KS#244	50	male	23.875	1520	5.190	2.754	3.761	0.740
KS#274	59	male	22.948	2300	1.032	9.591	1.562	0.891
Avg. (mean ± SD)	58.400 ± 6.877	-	22.213 ± 3.410	1676.000 ± 403.150	1.767 ± 2.105	18.584 ± 14.313	3.817 ± 1.732	1.860 ± 1.092
P NS vs. KS	0.852	0.999	0.722	0.783	0.738	0.015	0.002	0.020

2.   Cell viability of HK-2 cells treated by H_2O_2, NaOx, COM, KS and NS urine

HK-2 cell survival after treated with H_2O_2, NaOx, COM, KS and NS urine were investigated. The cells were treated with varied concentrations of H_2O_2 (3.125-50 µM), NaOx (112.5-1800 µM) and COM (3.125-50 µg/cm^3) for 72 h. The result showed that increased concentration of these stress inducers decreased cell survival. HK-2 cell survival was evidently decreased at 50 µM H_2O_2, 1800 µM NaOx and 50 µg/cm^3 COM compared with the untreated control (Figure 12). The effect of KS and NS urine (varied between 2.5 and 40% v/v) on HK-2 cell survival was also investigated. Obvious reduction of viability of HK-2 cell treated with NS urine was found at 40% v/v (Figure 13), while for KS urine treatment was found at 20% v/v, except in the case of KS#233 (Figure 14). This result indicated that KS#233 urine was highly toxic to HK-2 cells compared with other urine samples. It induced both senescence and cell death. Perhaps, it was due to the fact that KS#233 urine had higher concentrations of oxalate and other lithogenic factors than the other samples. Quantitative measurement of MTT assay is shown in Appendix 1.

In this study, we decided to use the working concentrations of H_2O_2, NaOx, COM, KS urine and NS urine for further experiments at 25 µM, 900 µM, 25 µg/cm^3, 10% v/v and 10% v/v, respectively. The main reason for choosing these concentrations for further experiments was that these concentrations were the minimum concentrations that could induce senescent phenotype in HK-2 cells, and had the lowest toxic effect to the cells.
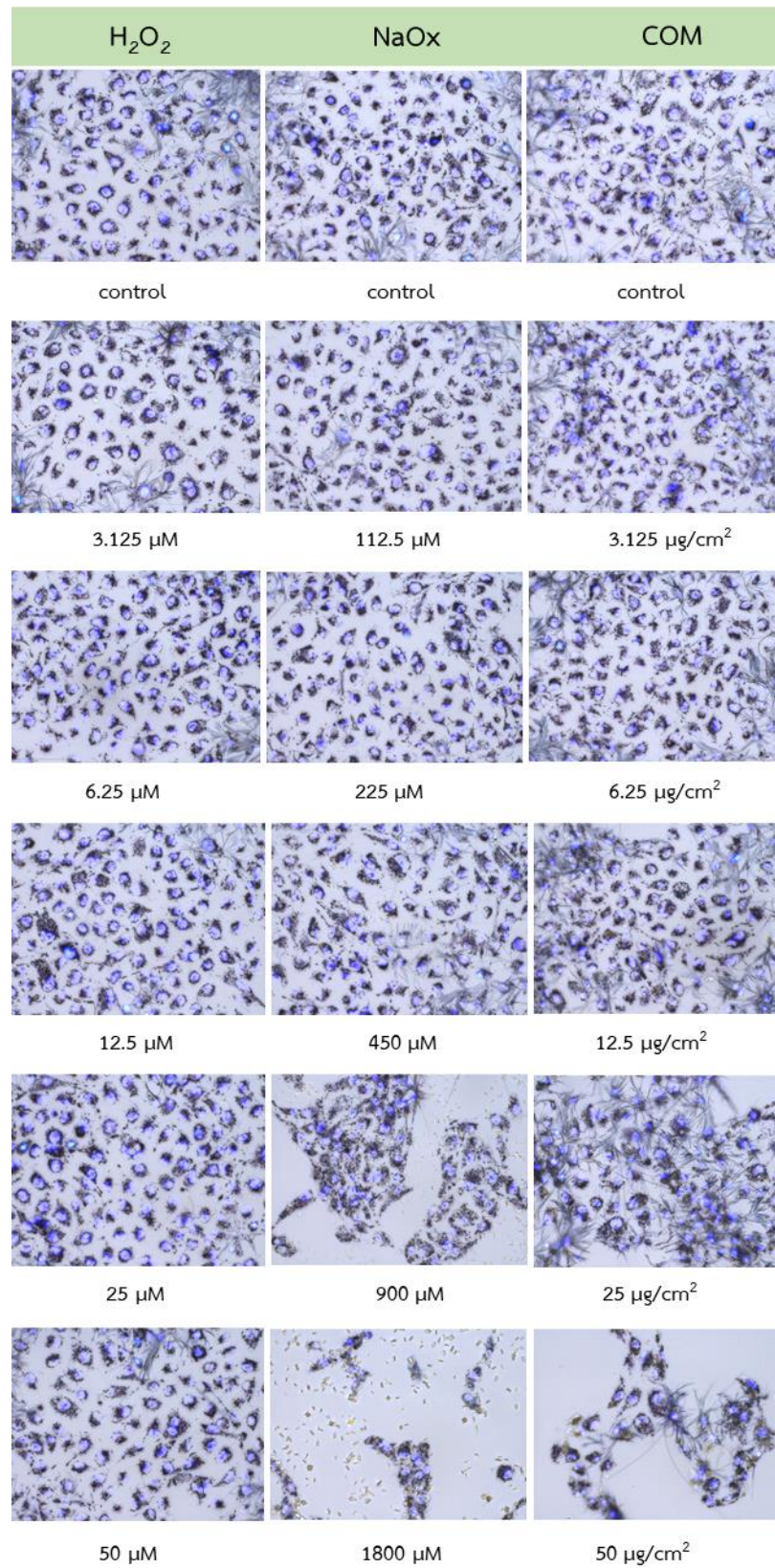
Figure 12. The viability of HK-2 cells treated with varied concentrations of H_2O_2, NaOx and COM. Nuclei were stained with DAPI (blue). Magnification x400.
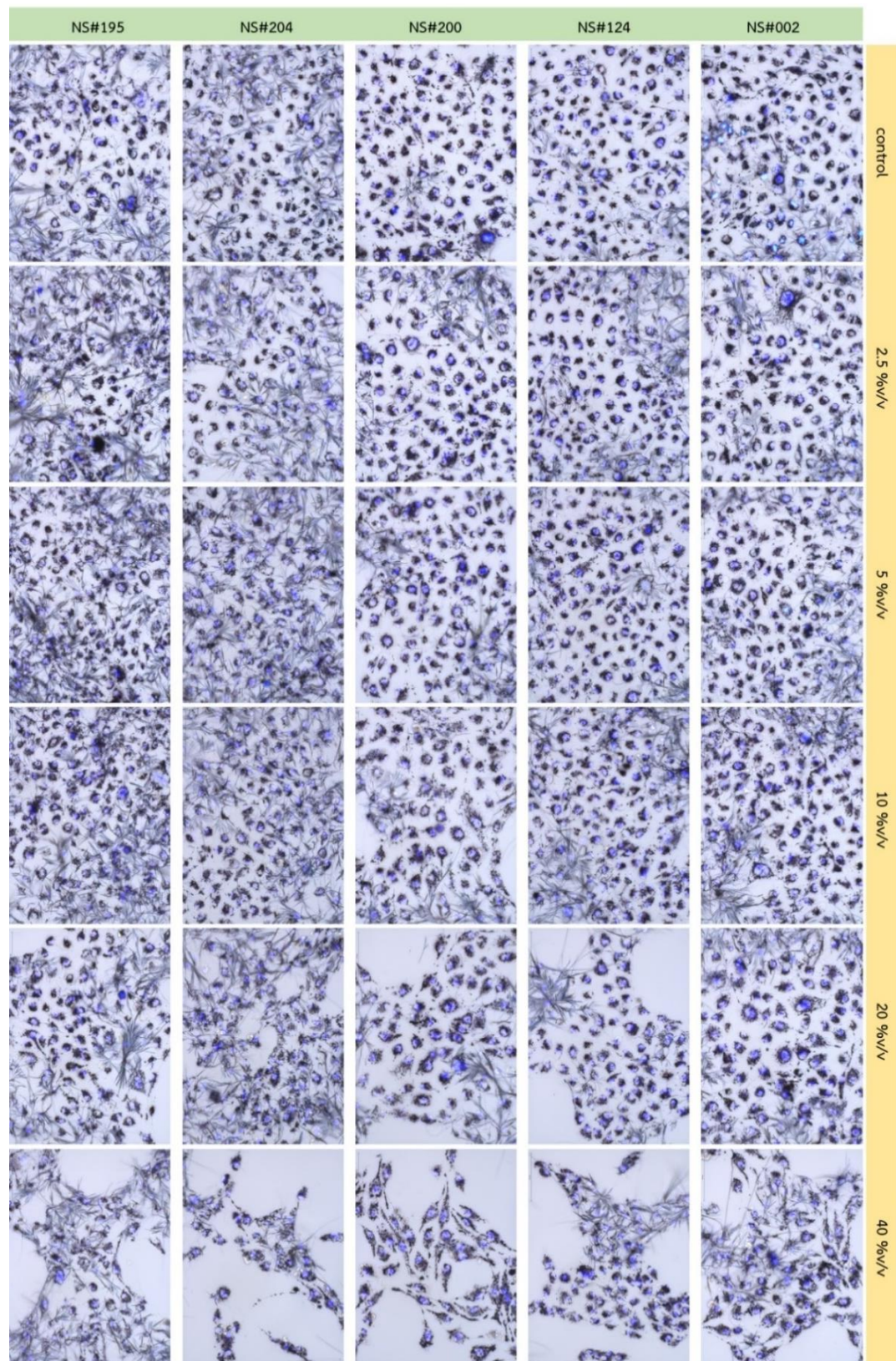
Figure 13. The viability in HK-2 cells treated with varied concentrations of 5 NS urine samples. Nuclei were stained with DAPI (blue). Magnification x400.
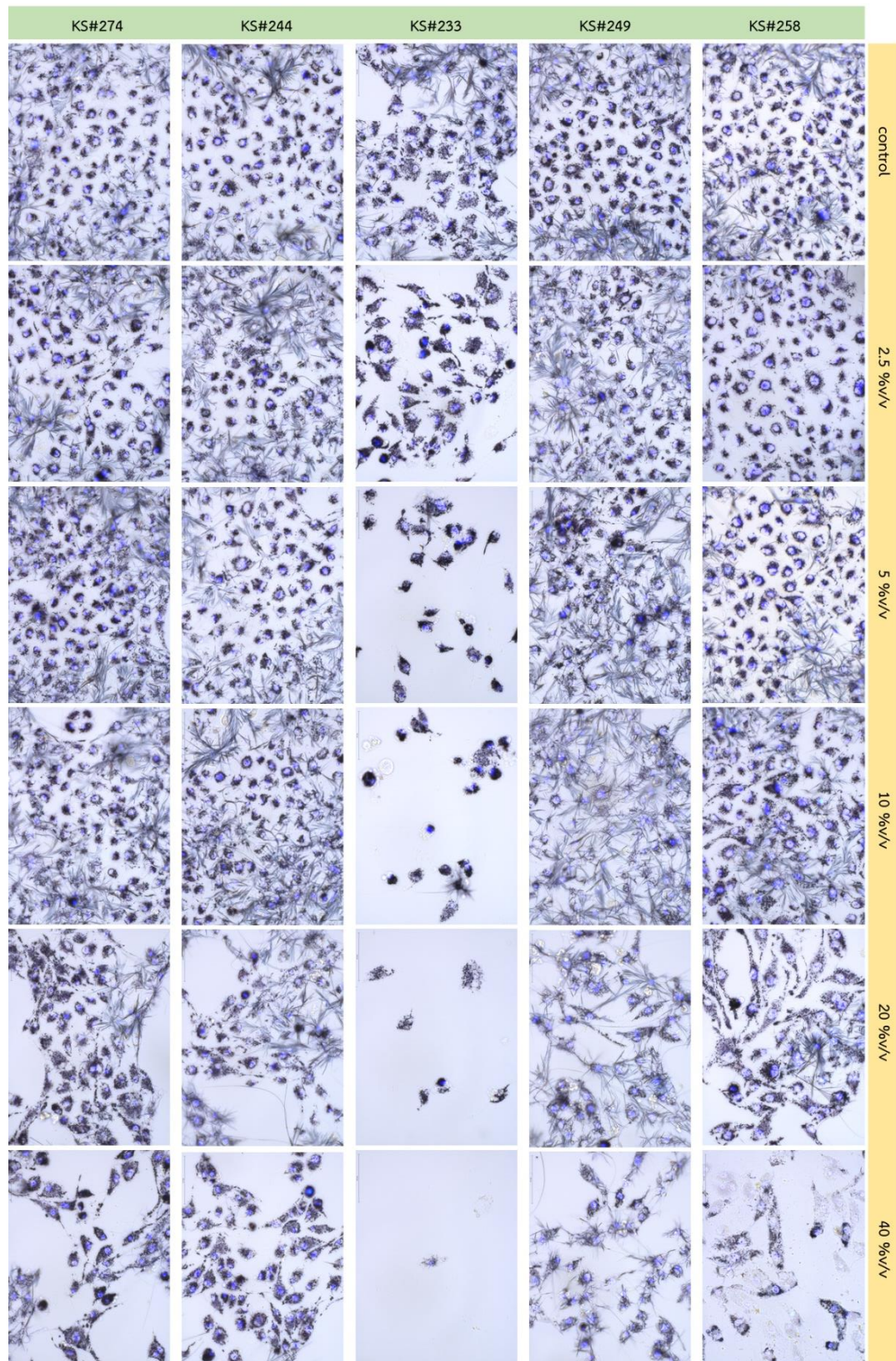
Figure 14. The viability in HK-2 cells treated with varied concentrations of 5 KS urine samples. Nuclei were stained with DAPI (blue). Magnification x400.

3.   H$_2$O$_2$, NaOx, COM, KS and NS urine induced premature senescence in HK-2 cells

Our previous study showed that treatment with 20 µM H$_2$O$_2$ for 10 days induced cellular senescence in HK-2 cells (135). In this study, we tested if H$_2$O$_2$ could induced premature senescence in HK-2 cells in the shorter period of time (3 days). We found that SA-βgal positive cells (blue ageing cells) in HK-2 cells treated with H$_2$O$_2$ (for 72 h) were highly increased compared with the untreated control (Figure 15). The result suggested that 3-day intervention could increase premature senescence in HK-2 cells similar to the 10-day intervention shown in our previous study (135). In addition to p16-mediated SIPS, we extended the investigation to other mechanism asking if this 3-day intervention could also induce cellular senescence through telomere shortening.

Since oxalate and COM were known to induce oxidative stress (63) and cell injury, we further asked if these CaOx lithogenic factors could also induce the premature senescence in HK-2 cells like H$_2$O$_2$ did. The result demonstrated that SA-βgal positive cells were significantly increased in HK-2 cells treated with NaOx and COM compared with untreated control (Figure 15). Then, the effect of KS and NS urine on induction of HK-2 cell senescence was investigated. After 3-day treatment, that the number of senescent cells were obviously increased in HK-2 cells treated with KS compared with NS urine and control (Figure 16). After that, we measured percentage of senescent cells in each treatment condition, and the result shown that senescent cells were significantly increased in HK-2 cells treated with H$_2$O$_2$, oxalate, COM and KS urine compared with untreated control and NS urine (Figure 17).

Oxidative stress inducers including H$_2$O$_2$, NaOx and COM could induce premature senescence in HK-2 cells according to our previous study (135), and oxidative stress largely contributed to the progression of age-related diseases oxidative stress (136, 137). In this study, we firstly demonstrated that KS urine triggered SIPS in HK-2 cells similar to H$_2$O$_2$, NaOx and COM. It might be possible that the lithogenic factors presented in the KS urine were responsible for the SIPS induction in HK-2 cells.
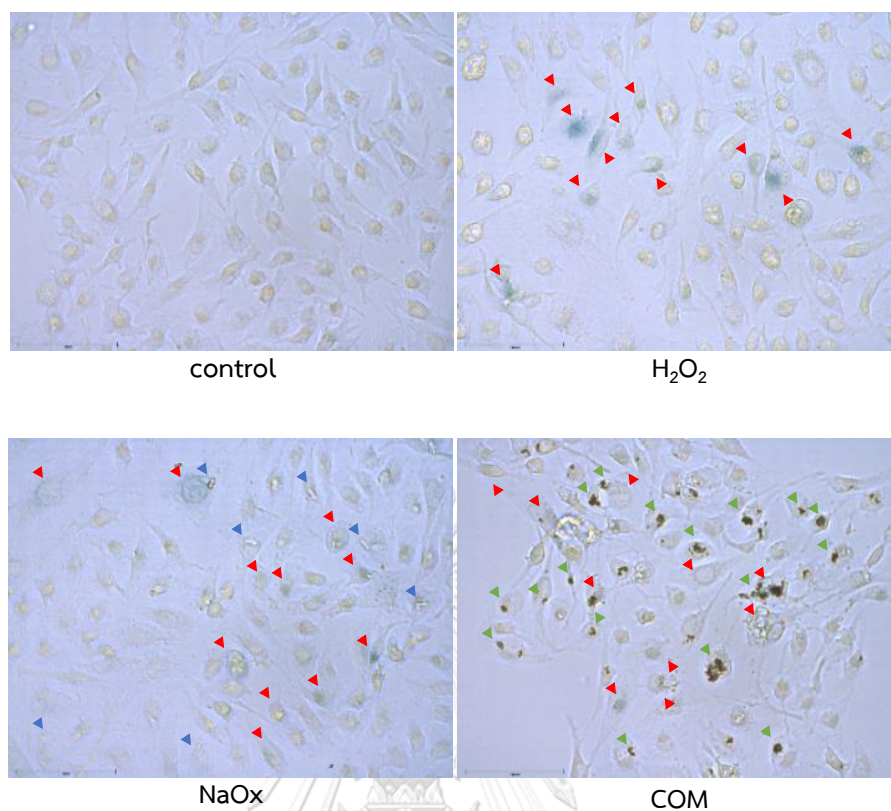
Figure 15. The morphology number of induced senescent cells in HK-2 cells treated with H_2O_2, NaOx and COM (x400 magnification). Red, blue and green arrowheads indicate SA-βgal positive cells, crystals formed in the NaOx-treated condition and the added COM crystals, respectively.
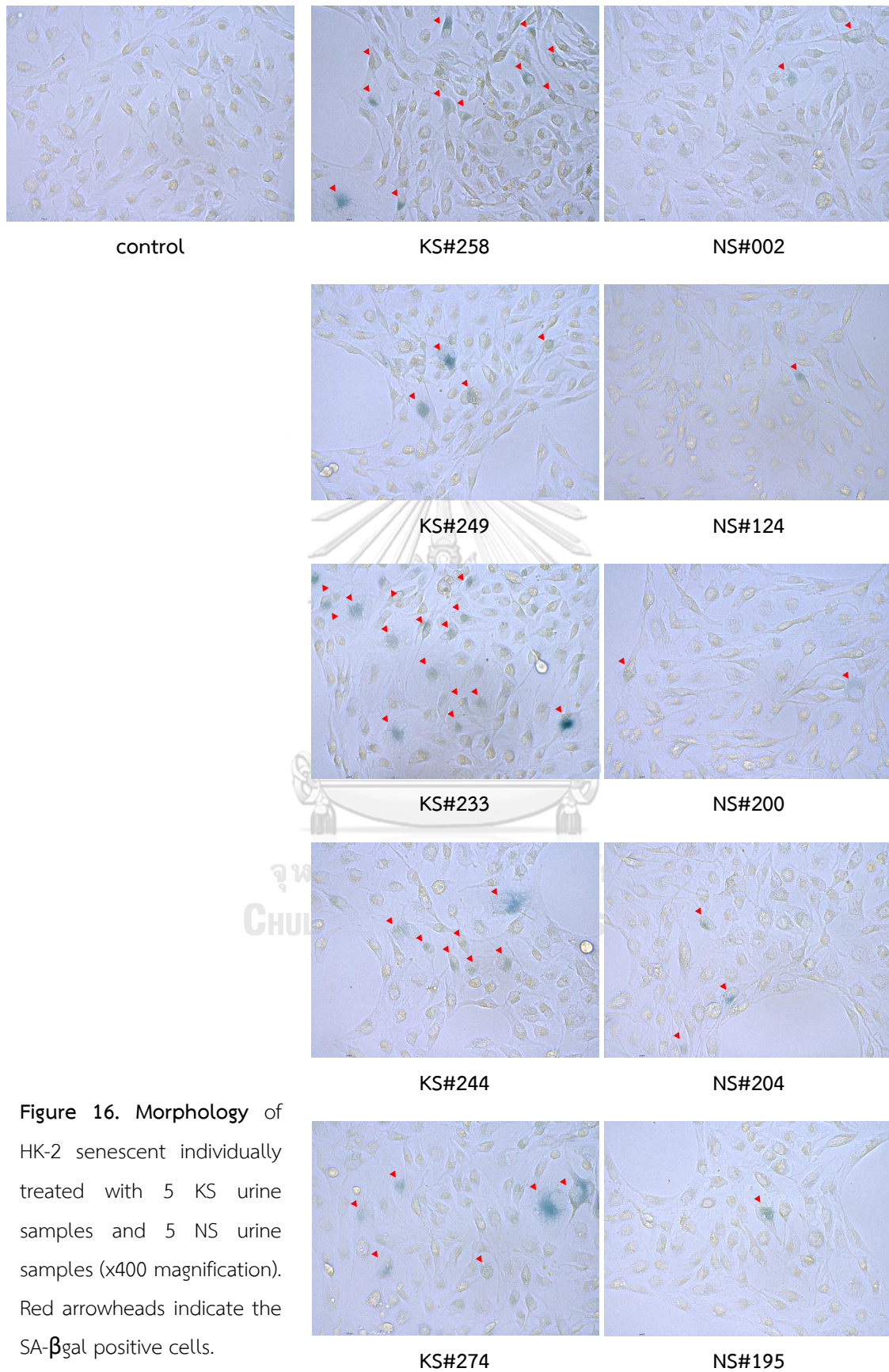
Figure 16. Morphology of HK-2 senescent individually treated with 5 KS urine samples and 5 NS urine samples (x400 magnification). Red arrowheads indicate the SA-βgal positive cells.

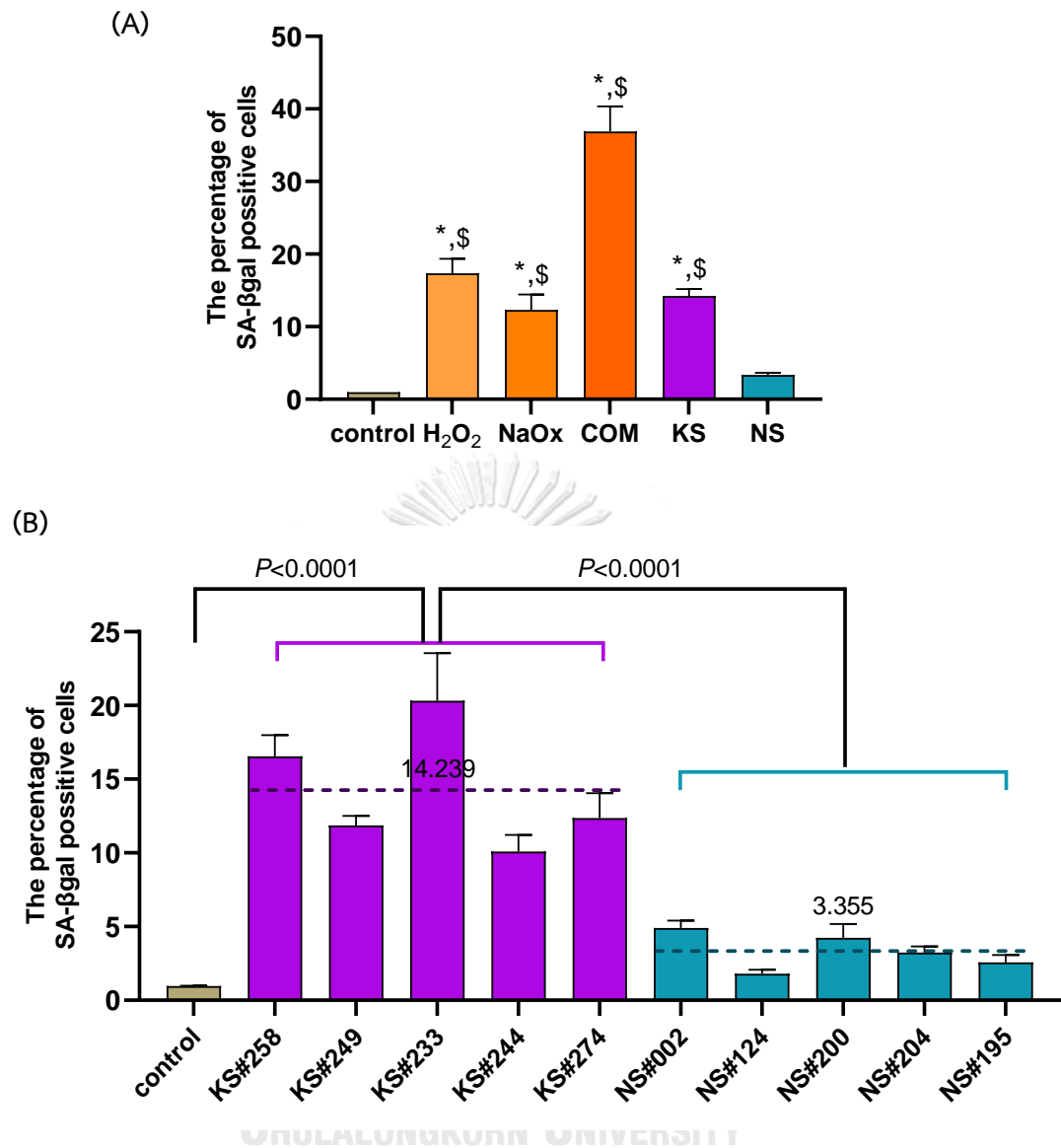**Figure 17.** The percentage of HK-2 senescent cells. (A) HK-2 cells were treated with H_2O_2, NaOx, COM, KS and NS urine. (B) Individual senescent data of each treatment of KS and NS urine. Dash line and number indicate mean in each group. *$P<0.05$ vs. control, $ $P<0.05$ vs. NS.

4.   H$_2$O$_2$, NaOx, COM, KS urine and NS urine induced oxidative stress in HK-2 cells

Our data shown that H$_2$O$_2$, NaOx, COM and KS urine could induce premature senescence in HK-2 cells. We hypothesized that H$_2$O$_2$, NaOx, COM and KS urine induced oxidative stress in HK-2 cells that further resulted in premature senescence. Protein carbonylation and TAC (oxidative stress markers) were determined after 3-day exposure of H$_2$O$_2$, NaOx, COM, KS and NS urine to HK-2 cells.

We found that protein carbonyl contents in HK-2 cells treated with H$_2$O$_2$, NaOx, COM and KS urine were significantly increased compared with the untreated control and NS urine (Figure 18A).

In contrast, TAC was significantly decreased in HK-2 cells treated with H$_2$O$_2$ compared with untreated control. Moreover, TAC was significantly decreased in HK-2 cells treated with NaOx, COM and KS urine compared with untreated control and NS urine (Figure 19A).

In this study, the increase in protein carbonylation and decrease in TAC were found in HK-2 cells treated with H$_2$O$_2$, NaOx, COM and KS urine. H$_2$O$_2$ is a well-known ROS that directly induces oxidative stress and premature senescence, as reported in many cell types such as endothelial cells (113, 138). The result of this study confirmed that NaOx and COM were capable of inducing oxidative stress and oxidative damage (139). Association of increased oxidative stress with aging phenotype were demonstrated in chronic kidney disease (140). The well-known mechanism of stress-induce premature senescence by oxidative stress is p16 overexpression. Although in the experiment we did not use antioxidant to inhibit oxidative stress to confirm that premature senescence was truly induced through oxidative stress, we did measure the oxidatively modified products and it was reasonable to believe that H$_2$O$_2$, NaOx, COM and KS urine induced premature senescence in HK-2 cells via induction of oxidative stress.

(A)

(B)
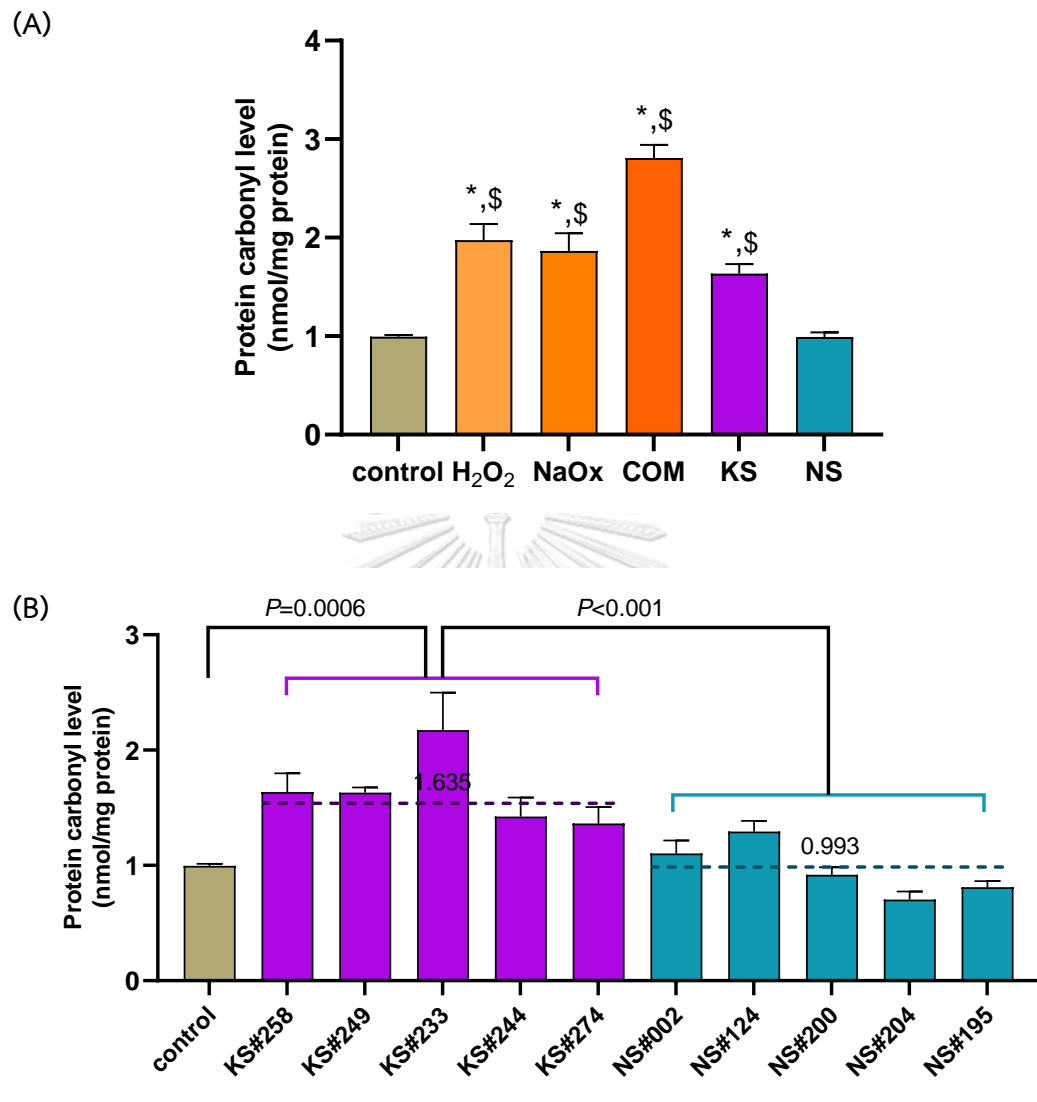
Figure 12. Protein carbonyl levels in HK-2 cells treated with H_2O_2, NaOx, COM, KS urine and NS urine. (A) Overall protein carbonyl levels in HK-2 cells induced by H_2O_2, NaOx, COM, KS urine and NS urine (B) Individual data of protein carbonyl in each urine treatment. Dash line and number indicate mean in each group. *$P<0.05$ vs. control, $ $P<0.05$ vs. NS.

(A)

(B)
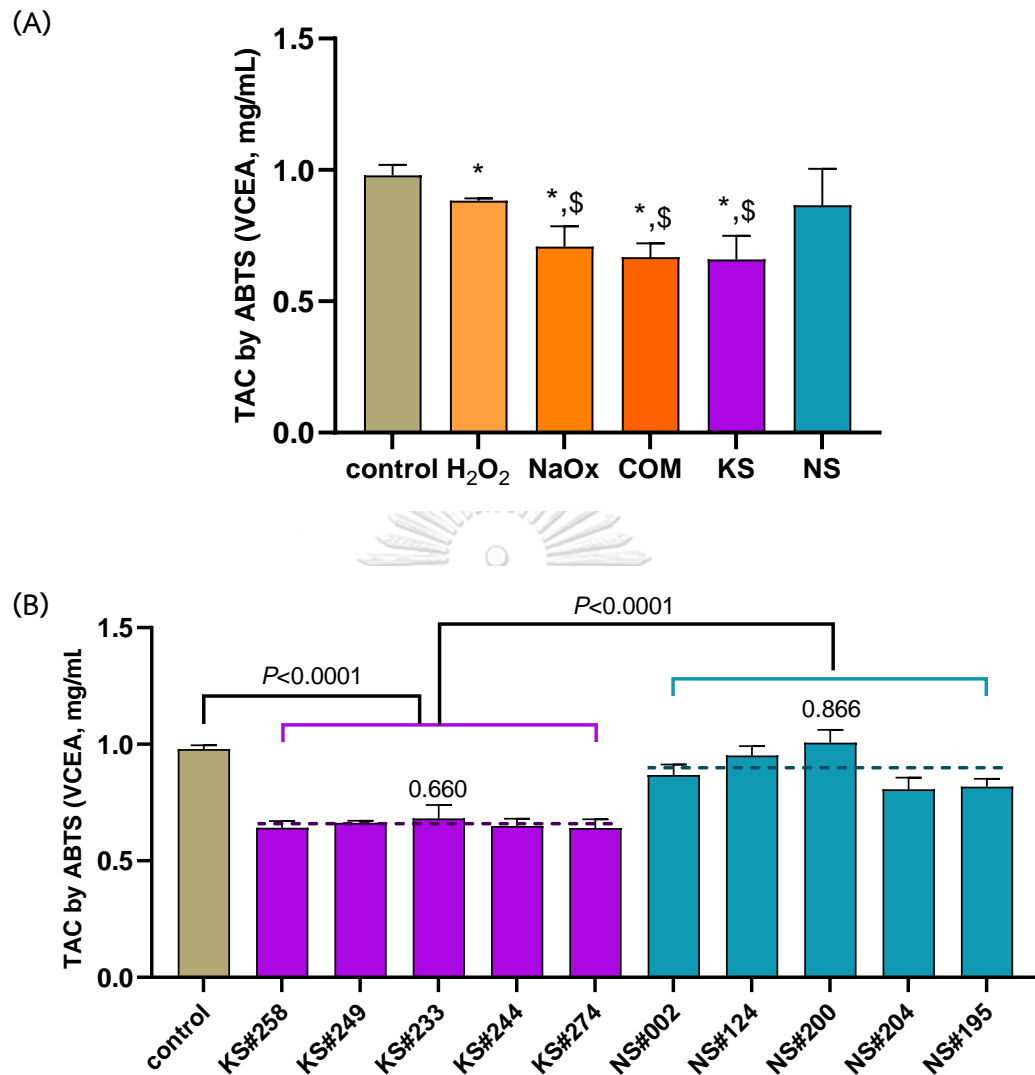
Figure 13. TAC in HK-2 cells treated with H_2O_2, NaOx, COM, KS urine and NS urine. (A) Overall TAC

in HK-2 cells induced by H_2O_2, NaOx, COM, KS urine and NS urine

(B) Individual data of TAC in each urine treatment. Dash line and number indicate mean in each

group. *$P<0.05$ vs. control, $ $P<0.05$ vs. NS.

5. **Premature senescence induced by H$_2$O$_2$, NaOx, COM and KS urine associated with increased p16 expression in HK-2 cells**

Our present data clearly demonstrated that H$_2$O$_2$, NaOx, COM and KS caused oxidative stress and premature senescence in HK-2 cells. Previous study by Liu Et al. showed that oxidative stress induced p16 overexpression (141). We asked if p16 was upregulated in the premature senescent cells. After 72 h, p16 expression was detected in each treatment condition using immunocytofluorescence staining. The result showed that p16 expression was highly increased in HK-2 cells treated with H$_2$O$_2$, NaOx, COM and KS urine compared with the untreated control and NS urine (Figure 20A). Interestingly, our double staining of SA-bgal and p16 immunocytofluorescence revealed that p16 was exclusively upregulated in the SA-bgal positive cells, suggested that the premature senescence was mediated through p16 function. The expressionp16 protein expression in HK-2 cells treated with H$_2$O$_2$, NaOx and COM were clearly greater than the untreated control, but in KS urine and NS urine treatments it was comparable to the control. (Figure 20B).

The immunofluorescent staining clearly convinced that p16 was overexpressed in the senescent HK-2 cells exposed to H$_2$O$_2$, NaOx, COM and KS urine. Liu Et al. demonstrated that oxidative stress induced in renal tubular epithelial cells led to premature senescence and p16 overexpression (141). The present result of p16 immunocytofluorescence staining and western blot in NS urine were not well correspondence. This may be due to many reasons. One could be the invalid result of western blot, indicated by the bands of GAPDH that were not constantly and equally expressed in all samples. It is strongly suggested that western blot must be repeated until the reproducible result is obtained. In addition, immunocytofluorescence staining of all other individual urine samples must be carried out.

(A)

(B)
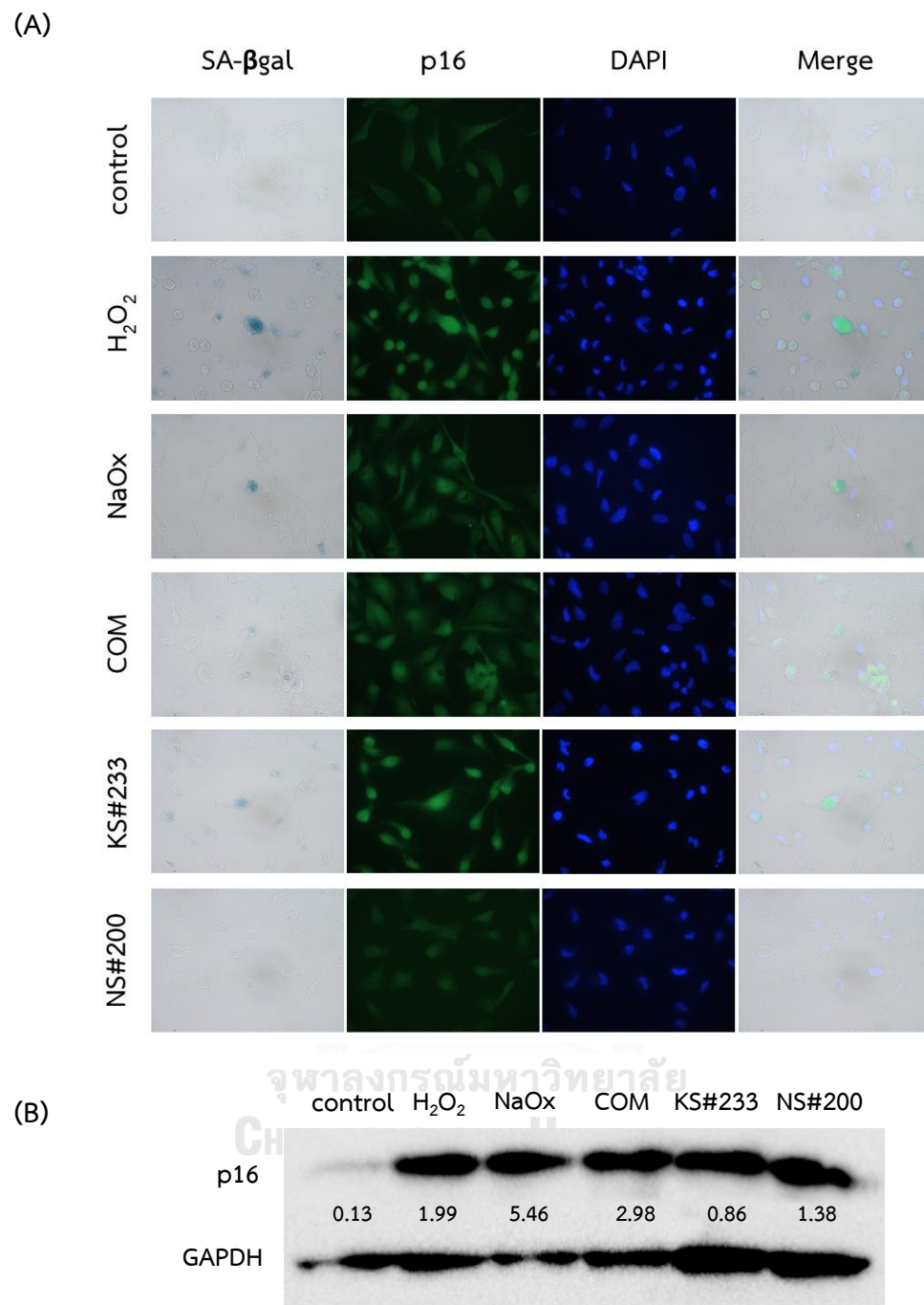
Figure 14. Double staining of SA-bgal staining and immunocytofluorescence showing association of premature senescence with p16 overexpression in HK-2 cells treated with H_2O_2, NaOx, COM, KS urine and NS urine. Magnification x600.

(A) SA-βgal staining for visualizing premature senescence cells and immunocytofluorescence staining of p16 (green). Nuclei were labeled by DAPI (blue). Expression of p16 was specifically upregulated in the senescent cells. (B) Western blot for detection ofp16 protein expression using GAPDH as loading control. Relative density normalized to GAPDH are shown in numbers.

6. **H$_2$O$_2$, NaOx, COM, KS and NS urine induced telomere shortening in HK-2 cells**

Evidence in coronary artery disease that are aging-associated disease shows that decreased in telomere length is caused by oxidative DNA damage (8-hydroxyl deoxyguanosine (8-OHdG)) (142). Our data showed that H$_2$O$_2$, NaOx, COM and KS urine resulted in oxidative stress in HK-2 cells for 72 h. We hypothesized that H$_2$O$_2$, NaOx, COM and KS urine could induce telomere shortening thought oxidative stress in HK-2 cells. After 3-day treatment with H$_2$O$_2$, NaOx, COM, KS urine and NS urine, RTL was measured using real-time qPCR. We found that the RTL was significantly decreased in HK-2 cells treated with H$_2$O$_2$, NaOx, COM and KS urine compared with the untreated control and NS urine (Figure 21A). The result indicated that decreased telomere length was a consequence of increased oxidative stress in HK-2 cells after treated with H$_2$O$_2$, NaOx, COM and KS urine. Telomere shortening is known to be correlated with SA-βgal activity (120). Study in human retinal pigment epithelial cells showed that senescent state of these cells had increased SA-βgal activity, and at the same time telomere length was decreased from 10 kb to 4 kb (120). Increase in SA-βgal activity is correlated with replicative senescence through telomere shortening (120). Telomeres are the G-rich region of chromosome that are sensitive for ROS attack to form 8-oxoguanine leading to oxidative DNA damage. Repairing the oxidative telomeric DNA is difficult because telomeres contain the shelterin complex (97). The accumulation of oxidative DNA damage leads to instability of T-loop formation and telomere shortening, and the critical shortening of telomere subsequently leads to cellular senescence. Although we did not measure oxidative DNA lesions in this study, our previous study demonstrated that HK-2 cells treated with COM had increased 8-OHdG lesions (143). In addition, we previously reported that 8-OHdG level in the urine of KS patients was higher than that in the NS urine (67).
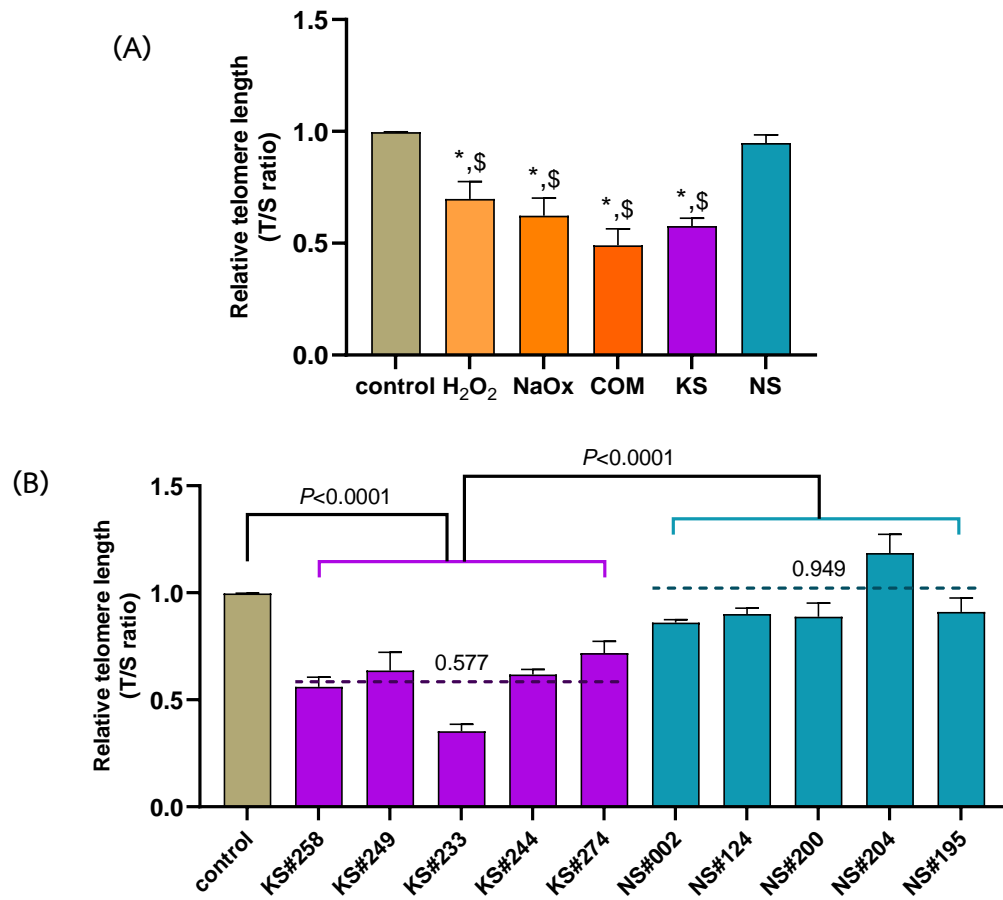
Figure 15. The RTL in HK-2 cells treated with H_2O_2, NaOx, COM, KS urine and NS urine.
(A) The RTL in HK-2 cells induced by H_2O_2, NaOx, COM, KS urine were significantly shorter than control and NS urine. (B) Individual data of RTL of each urine treatment. Dash line and number indicate mean in each group. *$P<0.05$ vs. control, $ $P<0.05$ vs. NS.

7.   The mRNA expression of shelterin complex mRNA in HK-2 cells treated with H$_2$O$_2$, NaOx, COM, KS urine and NS urine

After 3-day intervention, expression of shelterin complex mRNA were measured. Expression of TRF1 mRNA was significantly decreased in HK-2 cells treated with H$_2$O$_2$ compared with untreated control and NS urine. In contrast, TRF1 mRNA expression was significantly increased in HK-2 cells treated with COM compared with the untreated control and NS urine. TRF2 expression was significantly decreased in HK-2 cells treated with H$_2$O$_2$ and NaOx compared with untreated control. Furthermore, POT1 expression was significantly decreased in HK-2 cells treated with H$_2$O$_2$, NaOx and COM compared with untreated control and NS urine (Figure 22A).

Expression of TRF1 mRNA in HK-2 cells treated with KS urine was significantly decreased compared with the NS urine treatment. Both TRF2 and POT1 mRNA expression were significantly decreased in HK-2 cells treated with KS urine compared with untreated control and NS urine (Figure 22A).

The length of telomere is regulated and protected by shelterin complex, and there are six-protein components in this complex including TRF1, TRF2, TIN2, POT1, TPP1 and RAP1 (71, 72). Previous evidence showed that oxidative stress caused reduced expression of shelterin mRNA, especially TRF1, TRF2 and POT1 (134). In this study, we investigated the effect of oxidative stress on expression of shelterin complex mRNA in HK-2 cells treated with H$_2$O$_2$, NaOx, COM and KS urine. The expression of TRF1 mRNA, telomere elongation and T-loop formation protein (144-146), was decreased in HK-2 cells treated with H$_2$O$_2$, NaOx and KS urine. This was corresponded with the previous study in human hepatocytes exposed to TiO$_2$-NPs (134). In contrast, the expression of TRF1 mRNA in HK-2 cells treated with COM was exceptionally elevated. We assumed that COM, as an insoluble form of oxalate, may interfere the expression of shelterin complex especially TRF1 differently from the soluble oxalate NaOx. Even though TRF1 mRNA was elevated, the other shelterin proteins (TRF2 and POT1) were decreased. Therefore, we thought that the complete functional shelterin complex was decreased and stabilization of telomeric end was compromised. The TRF2 acts to help invasion of G-rich overhang to dsDNA (144, 145). TRF2 was decreased in HK-2 cells treated with H$_2$O$_2$, NaOx, COM and KS urine. We speculate that low expression of TRF2

mRNA promotes activation of ATM signaling pathway that leads to p53 activation, cell cycle arrest and cellular senescence, respectively (147). However, this speculation requires further experimental proof. POT1 is a ssDNA binding protein. Its mRNA expression was much lower than TRF1 and TRF2 mRNA in HK-2 cells treated with H_2O_2, NaOx, COM and KS urine. Reduction of POT1 might lead activation of ATR signaling pathway through replication protein A that further leads to p53 activation, cell cycle arrest and cellular senescence (148). In conclusion, our results suggest that low expression of shelterin complex mRNA in HK-2 cells treated with H_2O_2, NaOx, COM and KS urine are induced by oxidative stress that consequently causes instability of T-loop formation of shelterin complex leading to DNA damage response pathway activation and cellular senescence.

(A)
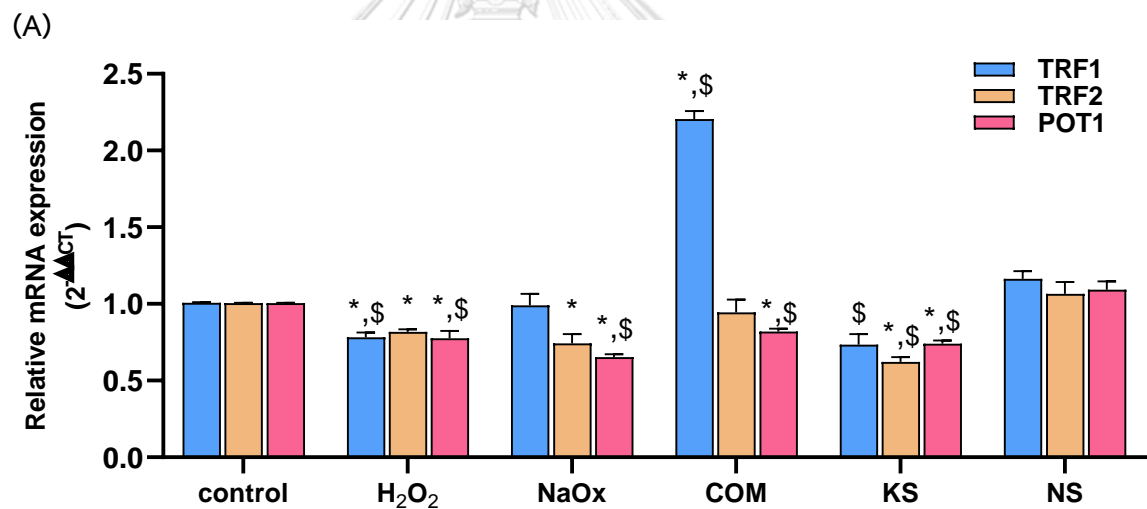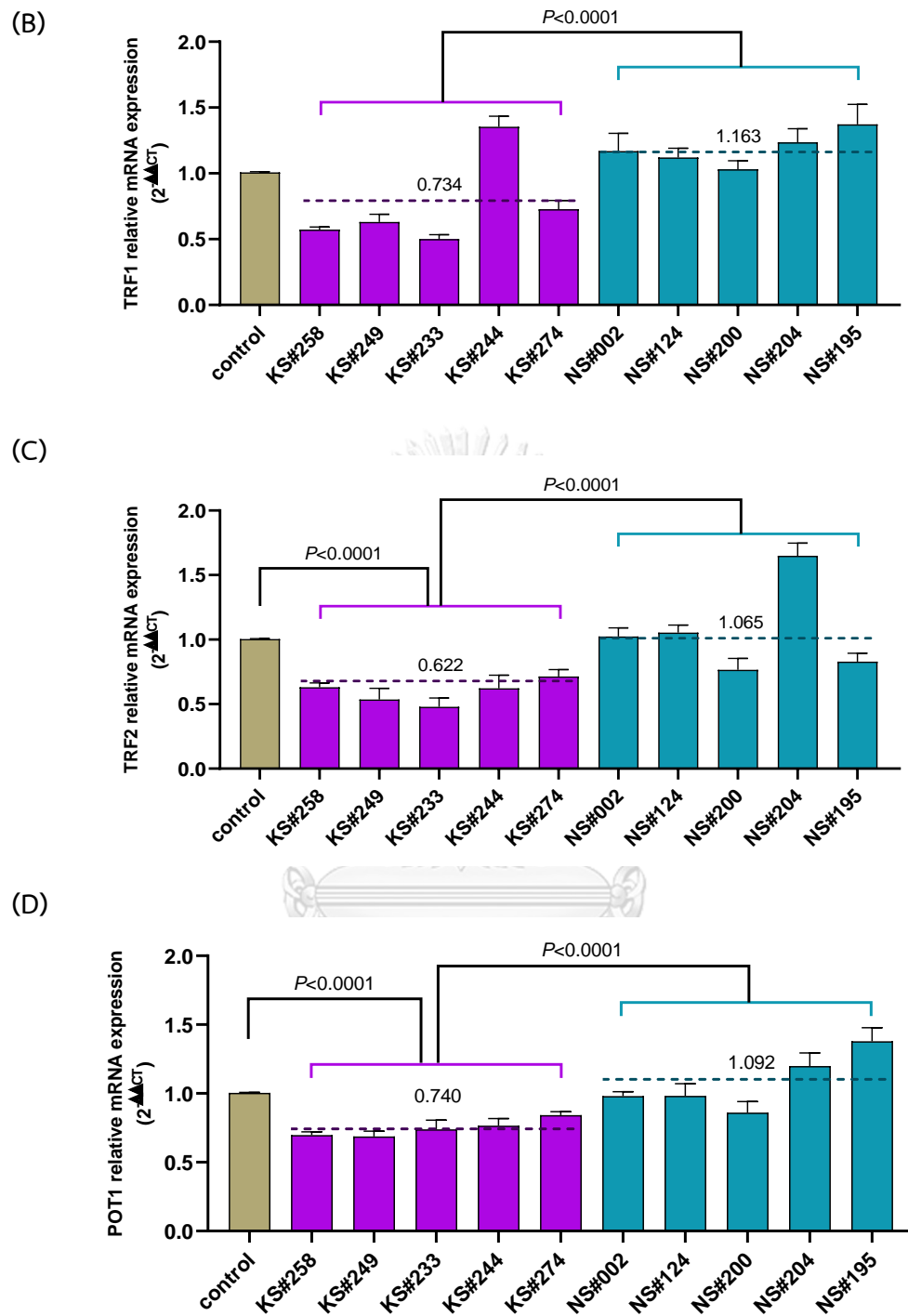
Figure 16. The relative mRNA expression of TRF1, TRF2 and POT1 in HK-2 cells treated with H_2O_2, NaOx, COM, KS urine and NS urine. (A) Overall mRNA expression of TRF1, TRF2 and POT1 in HK-2cells induced by H_2O_2, NaOx, COM, KS urine and NS urine. Individual data of TRF1, TRF2 and POT1 transcript expression are shown in (B), (C) and (D), respectively. Dash line and number indicate mean in each group. *$P<0.05$ vs. control, $ $P<0.05$ vs. NS.

Discussion and Conclusion

In this study, we aimed to investigate the effect of lithogenic factors including oxalate, COM and KS urine on telomere shortening and cellular senescence in HK-2 cells via oxidative stress. Exposure of kidney cells, especially tubular cells, to oxalate and CaOx promotes stone formation through induction of oxidative stress and renal injury (63, 149). Urine from KS patients is also known to induce oxidative stress in renal tubular cells (150). Our present results clearly demonstrated that oxalate, COM and KS urine were capable of inducing oxidative stress, telomere erosion and premature senescence in HK-2 cells.

HK-2 cells treated with H_2O_2 exhibited an increase in SA-βgal activity was consistent with other studies in fibroblasts (151, 152), endothelial cells (153, 154) and kidney tubular cells (140, 155), underlined that ROS was a known SIPS inducer. The novel finding gained from this study was that HK-2 cells treated with oxalate (soluble form of CaOx crystals) and COM (toxic form of CaOx crystals) had increased SA-βgal activity compared with control, indicating that oxalate and COM were also inducers of SIPS. To get a closer link to the clinical setting, we tested whether urine from KS patients was able to induce SIPS, and the result revealed that the KS urine did like oxalate and COM. This suggested that renal tubular cells in KS patients that persistently exposed to lithogenic milieu aged faster than those in NS subjects. How and to what extent this premature senescence contributes to the pathogenesis of CaOx stone development remain to be elucidated.

Studies in kidney tubular cells (140) and endothelial cells (138) demonstrated that H_2O_2 exposure could produce free radicals leading to oxidative stress. Oxidative stress caused by exposure of HK-2 cells to oxalate and COM was also reported (63). Our data showed that protein carbonyl levels was increased, but TAC was decreased in HK-2 cells treated with H_2O_2, NaOx, COM and KS urine relative to control and NS urine. These results confirmed that lithogenic substances and KS urine actually injurious by inducing oxidative damage that was well agreed with the previous studies in cell culture and KS patients (156-161).

Previous studies showed that oxidative stress induced SIPS via p16 [INK4a] overexpression and increased DNA damage at the chromosome ends (called telomere) (58-62). Upon an activation of p16 [INK4a], CDK 2/4 is inhibited that further suppresses phosphorylation of pRb resulting in pRb activation, inactivation of E2F, inhibition of S-phase gene expression and induction of cellular growth arrest, respectively. In this study, H_2O_2, NaOx, COM and KS urine exposures upregulated the expression of p16 [INK4a] in HK-2 cells that was agreed well with the well-accepted concept of oxidative stress-induced p16-dependent senescence. In addition, in this study we clearly showed that the senescent cells remarkably expressed p16 protein compared with the non-senescent cells.

Effect of ROS on telomere length and shelterin complex gene expression was investigated in this study. Telomeres are the ends of chromosome that rich in guanine (G) content that is highly susceptible for oxidative modification. The accumulation of oxidative DNA damage leading to telomere shortening, and the critical shortening of telomere leading to cellular senescence. In this study, we corroborated that H_2O_2 decreased telomere length in HK-2 cells consistent with the findings in fibroblasts (97, 162). Importantly, telomere length was decreased in HK-2 cells treated with NaOx, COM and KS urine. So far, there has been no report about effect of lithogenic factors on telomere attrition. This is the first report showing that oxalate, COM and urine obtained from CaOx stone patients induce telomere shortening in the renal tubular cells.

We further investigated what the possible mechanism of lithogenic factors (oxalate/COM/KS urine)-induced telomere shortening. Shelterin complex is six-telomeric binding protein that regulates length of telomere and prevents chromosome ends from DNA strand break and DNA damage response pathway (163). Low expression of shelterin complex and accumulation of oxidative DNA lesions at telomeric ends leads to telomere shortening, activation of DNA damage response pathway and cellular senescence (164). The main proteins of shelterin complex are TRF1, TRF2 that bind dsDNA and act in telomere elongation (165) and T-loop formation (166). The other key protein is POT1 that functions as ssDNA binding protein and inhibits DNA damage response pathway (167). In this study, TRF1, TRF2, POT1 expression were decreased in

HK-2 cells treated with H_2O_2, NaOx and COM. Notably, exposure of HK-2 cells to KS urine caused decreases in TRF1, TRF2, POT1 mRNA expression. Although the protein levels of TRF1, TRF2 and POT1 were not measured, it was suggested that shortening of telomeric DNA by these oxidative stress inducing factors was at least in part mediated via downregulation of TRF1, TRF2, POT1 shelterin proteins.

The limitation of this study should be mentioned. Confirmation of lithogenic factors-induced SIPS through oxidative stress by supplementation with antioxidants was not performed in the present study. We anticipate that antioxidants will attenuate oxidative stress and that leads to inhibition of premature senescence. Oxidative DNA damage lesion (8-OHdG) at telomeres was not measured to support the hypothesis that oxidative lesions at telomeric end led to telomeric instability and shortening of telomeres. Additionally, the protein expression and localization of TRF1, TRF2 and POT1 were not investigated in this study. However, we have planned to carry out all of the mentioned experiments in future study.

In conclusion, to our knowledge we firstly demonstrated that oxalate, COM and CaOx stone urine induced cellular senescence, specifically SIPS, and telomere shortening in HK-2 cells. This senescent induction was likely mediated through oxidative stress and $p16^{INK4a}$ overexpression. Decreased expression of shelterin proteins, especially POT1, is at least in part responsible for telomere attrition. The results of the present study suggest that renal proximal tubular cells exposed to lithogenic factors, especially oxalate and COM are oxidatively injured, and that subsequently leads to telomere shortening and premature senescence. This induction of premature senescence might contribute to the development of CaOx calculi. Antioxidant intervention for attenuating ROS production and reducing oxidative stress might be clinically useful to decelerate ageing in renal tubular cells, and therefore reduce the risk of CaOx kidney stone disease.

APPENDIX

Appendix 1

Cell viability of NaOx and KS#233 urine treated in HK-2 cells

In this study, we investigated percent of viability of HK-2 cells treated with NaOx and KS#233 urine by MTT assay in 6-well plate. HK-2 cells were treated with 112.5-1800 µM NaOx and 2.5-20% v/v KS#233 urine for 72 h. The percent of cell viability was significantly decreased in 112.5-1800 µM NaOx-treated conditions compared with untreated control (Figure 23). For the KS urine treatment, the cell viability was significantly decreased in 5-20% v/v KS#233 urine-treated conditions compared with untreated control (Figure 24).
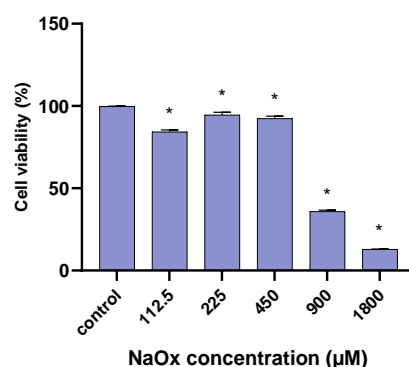
Figure 17. Cell viability (%) of HK-2 cells treated with 112.5-1800 µM NaOx measured by MTT assay. *$P < 0.05$ vs. control
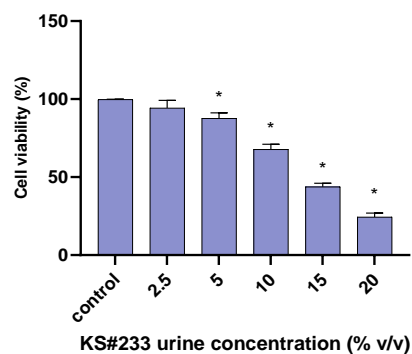
Figure 18. Cell viability (%) of HK-2 cells treated with 2.5-20% v/v KS#233 measured by MTT assay. *$P < 0.05$ vs. control

Appendix 2

Recipes of reagents used in this study

1.   **Reagents for MTT assay**

1.1   **10X PBS, pH 7.4**

-       Na_2HPO_4 (MW=141.98)   14.4 g

-       KCl (MW=74.44)   2 g

-       KH_2PO_4 (MW=136.08)   2.4 g

-       NaCl (MW=58.44)   80 g

-       Distilled water (DW)   700 mL

Adjust pH to 7.4 and adjust volume to 1 L with DW

1.2   **5 mg/mL 3-(4,5-dimethylthiazol-2-yl)-2,5-diphenyl tetrazolium bromide (MTT)**

-       MTT   5 mg

-       PBS   1 mL

-       Store at -20 ℃

1.3   **0.5 mg/mL MTT working solution**

-       5 mg/mL MTT in PBS   1 mL

-       Serum-free media   9 mL

2.   **Reagents for protein carbonyl assay**

2.1   **20% w/v Trichloroacetic acid (TCA)**

-       TCA   20 g

-       DW   100 mL

2.2   **10 mM 2,4-Dinitrophenylhydrazine (DNPH)**

-       DNPH (MW=198.14)   0.991 g

-       2N HCl   500 mL

2.3   **Ethanol: Ethyl acetate (ratio 1:1)**

-     Ethanol   100 mL
-     Ethyl acetate   100 mL

2.4   **Guanidine hydrochloride (GdmCl) (6 M GdmCl, 0.5 M potassium phosphate (KH_2PO_4), pH 2.5)**

-     GdmCl   286.6 g
-     KH_2PO_4 34.023 g
-     DW   300 mL

Adjust pH to 2.5 and adjust volume to 500 mL with DW

3.   **Reagents for ABTS assay**

3.1   **5 mM 2,2′-Azino-bis (3-ethylbenzothiazoline-6-sulfonic acid) (ABTS)**

-     ABTS (MW=584.7)   0.1372 g
-     PBS   50 mL

3.2   **2.5 mM 2,2′-Azobis(2-methylpropionamidine) dihydrochloride (AAPH)**

-     AAPH (MW=271.2)   0.0542 g
-     PBS   100 mL

4.   **Reagents for SA-βgal staining**

4.1   **100 mM Citric acid**

-     Citric acid (MW=210.14)   2.1014 g
-     DW   100 mL

4.2   **200 mM Sodium phosphate**

-     $NaH_2PO_4.H_2O$ (MW=137.99)   2.7598 g
-     DW   100 mL

4.3 **0.2 mM Citric acid/Na phosphate buffer**

- 100 mM Citric acid   36.85 mL
- 200 mM Sodium phosphate   63.15 mL

Adjust pH to 2.5

4.4 **100 mM Potassium hexacyanoferrate (III) $K_3[Fe(CN)_6]$**

- $K_3[Fe(CN)_6]$ (MW=422.39)   4.239 g
- DW   100 mL

4.5 **100 mM Potassium ferrocyanide $K_4[Fe(CN)_6]$**

- $K_4[Fe(CN)_6]$ (MW=329.25)   3.2925 g
- DW   100 mL

4.6 **5 M Sodium chloride (NaCl) ความเข้มข้น 5M**

- NaCl (MW=58.44)   14.61 g
- DW   50 mL

4.7 **1 M Magnesium chloride ($MgCl_2$)**

- $MgCl_2$ (MW=203.30)   10.165 g
- DW   50 mL

4.8 **20 mg/mL X-gal Solution**

- X-gal (MW=408.63)   0.2 g
- N, N-Dimethylaniline   20 mL

4.9 **Fixation solution**

- 37% Formaldehyde (vol/vol)   13.51 mL
- 50% Glutaraldehyde (vol/vol)   1 mL

Adjust volume to 250 mL with PBS

5.   **Reagents for Immunocytofluorescent staining**

5.1   **4% (w/v) Paraformaldehyde**

- Paraformaldehyde   4 g
- DW   100 mL

5.2   **0.5% Triton X-100 in PBS**

- Triton X-100   0.5 mL
- PBS   100 mL

5.3   **Non-specific blocking 10% Normal horse serum**

- Normal horse serum   1 mL
- PBS   9 mL

6. Reagents for western blots

6.1   **10x Running buffer**

- Tris-base   30 g
- Glycine   144 g
- SDS   10 g
- DW   1 L

6.2   **10x Transfer buffer**

- Tris-base   30.3 g
- Glycine   147.1 g
- DW   1 L

6.3   **10x TBS**

- Tri-base   61 g
- NaCl   87.6 g
- DW   1 L

Adjust pH to 7.6

6.4 **Mild stripping buffer**

-	Glycine	1.5 g
-	SDS	0.1 g
-	Tween 20	1 mL
-	DW	1 L

Adjust pH to 2

REFERENCES

1.   Yanagawa M, Kawamura J, Onishi T, Soga N, Kameda K, Sriboonlue P, et al. Incidence of urolithiasis in northeast Thailand. Int J Urol. 1997;4(6):537-40.

2.   Edvardsson VO, Indridason OS, Haraldsson G, Kjartansson O, Palsson R. Temporal trends in the incidence of kidney stone disease. Kidney Int. 2013;83(1):146-52.

3.   Sorokin I, Mamoulakis C, Miyazawa K, Rodgers A, Talati J, Lotan Y. Epidemiology of stone disease across the world. World J Urol. 2017;35(9):1301-20.

4.   Sigurjonsdottir VK, Runolfsdottir HL, Indridason OS, Palsson R, Edvardsson VO. Impact of nephrolithiasis on kidney function. BMC Nephrol. 2015;16:149.

5.   Alelign T, Petros B. Kidney Stone Disease: An Update on Current Concepts. Adv Urol. 2018;2018:3068365.

6.   Khan SR. Hyperoxaluria-induced oxidative stress and antioxidants for renal protection. Urol Res. 2005;33(5):349-57.

7.   Boonla C. Reactive Oxygen Species (ROS) in Living Cells: IntechOpen; 2018 [Available from: https://www.intechopen.com/books/reactive-oxygen-species-ros-in-living-cells/oxidative-stress-in-urolithiasis.

8.   Yang H, Fogo ABJJotASoN. Cell senescence in the aging kidney. 2010;21(9):1436-9.

9.   Shawi M, Autexier C. Telomerase, senescence and ageing. Mech Ageing Dev. 2008;129(1-2):3-10.

10.   Yu SL, Gan XG, Huang JM, Cao Y, Wang YQ, Pan SH, et al. Oxalate impairs aminophospholipid translocase activity in renal epithelial cells via oxidative stress: implications for calcium oxalate urolithiasis. J Urol. 2011;186(3):1114-20.

11.   Houben JM, Moonen HJ, van Schooten FJ, Hageman GJ. Telomere length assessment: biomarker of chronic oxidative stress? Free Radic Biol Med. 2008;44(3):235-46.

12.   Wang WJ, Cai GY, Chen XM. Cellular senescence, senescence-associated secretory phenotype, and chronic kidney disease. Oncotarget. 2017;8(38):64520-33.

13.   Campisi J. Cellular Senescence, Aging and Cancer. ScientificWorldJournal. 2001;1:65.

14.   Wang H, Ni J, Guo X, Zhou T, Ma X, Xue J, et al. Shelterin differentially respond to oxidative stress induced by TiO(2)-NPs and regulate telomere length in human hepatocytes and hepatocarcinoma cells in vitro. Biochemical and biophysical research communications. 2018;503(2):697-702.

15.   Swanson MJ, Baribault ME, Israel JN, Bae NSJBr. Telomere protein RAP1 levels are affected by cellular aging and oxidative stress. 2016;5(2):181-7.

16.   Wong JM, Collins K. Telomere maintenance and disease. Lancet. 2003;362(9388):983-8.

17.   Kurz DJ, Decary S, Hong Y, Erusalimsky JDJJocs. Senescence-associated (beta)-galactosidase reflects an increase in lysosomal mass during replicative ageing of human endothelial cells. 2000;113(20):3613-22.

18.   Campisi J. Senescent cells, tumor suppression, and organismal aging: good citizens, bad neighbors. Cell. 2005;120(4):513-22.

19.   Robertson WG, editor Renal stones in the tropics. Seminars in nephrology; 2003: Elsevier.

20.   Curhan GCJUCoNA. Epidemiology of stone disease. 2007;34(3):287-93.

21.   Sorokin I, Mamoulakis C, Miyazawa K, Rodgers A, Talati J, Lotan YJWJoU. Epidemiology of stone disease across the world. 2017;35(9):1301-20.

22.   Yoshida O, Terai A, Ohkawa T, Okada YJKi. National trend of the incidence of urolithiasis in Japan from 1965 to 1995. 1999;56(5):1899-904.

23.   Osther PJ. Epidemiology of kidney stones in the European Union. Urolithiasis: Springer; 2012. p. 3-12.

24.   Hesse A, Brändle E, Wilbert D, Köhrmann K-U, Alken PJEu. Study on the prevalence and incidence of urolithiasis in Germany comparing the years 1979 vs. 2000. 2003;44(6):709-13.

25.   Yanagawa M, Kawamura J, Onishi T, Soga N, Kameda K, Sriboonlue P, et al. Incidence of urolithiasis in northeast Thailand. 1997;4(6):537-40.

26.   More-krong P, Tubsaeng P, Madared N, Srisa-Art M, Insin N, Leeladee P, et al. clinical validation of urinary indole-reacted calcium oxalate crystallization index (icoci) test for diagnosing calcium oxalate urolithiasis. 2020;10(1):1-11.

27.   Romero V, Akpinar H, Assimos DGJRiu. Kidney stones: a global picture of prevalence, incidence, and associated risk factors. 2010;12(2-3):e86.

28.   Knoll T, Schubert AB, Fahlenkamp D, Leusmann DB, Wendt-Nordahl G, Schubert GJTJou. Urolithiasis through the ages: data on more than 200,000 urinary stone analyses. 2011;185(4):1304-11.

29.   Tosukhowong P, Boonla C, Ratchanon S, Tanthanuch M, Poonpirome K, Supataravanich P, et al. Crystalline composition and etiologic factors of kidney stone in Thailand: update 2007. 2007.

30.   Boonla C, Thummaborworn T, Tosukhowong P. Urolithiasis in Udon Thani Hospital: A rising prevalence of uric acid stone. 2006.

31.   Ogawa Y. Epidemiology of stone disease over a 40-year period in Japan. Urolithiasis: Springer; 2012. p. 89-96.

32.   Curhan GC, Willett WC, Rimm EB, Stampfer MJJJotASoN. Family history and risk of kidney stones. 1997;8(10):1568-73.

33.   Sritippayawan S, Borvornpadungkitti S, Paemanee A, Predanon C, Susaengrat W, Chuawattana D, et al. Evidence suggesting a genetic contribution to kidney stone in northeastern Thai population. 2009;37(3):141-6.

34.   Ngo TC, Assimos DGJRiu. Uric acid nephrolithiasis: recent progress and future directions. 2007;9(1):17.

35.   Zahid I, Bawazir A, Naser RJJoP, Phytochemistry. Plant based native therapy for the treatment of Kidney stones in Aurangabad (MS). 2013;1(6).

36.   Siener RJUr. Impact of dietary habits on stone incidence. 2006;34(2):131-3.

37.   Robertson W, Peacock MJN. The cause of idiopathic calcium stone disease: hypercalciuria or hyperoxaluria? 1980;26(3):105-10.

38.   Saepoo S, Adstamongkonkul D, Tosukhowong P, Predanon C, Shotelersuk V, Boonla CJCMJ. Comparison of urinary citrate between patientswith nephrolithiasis and healthy controls. 2009;53(1):51-65.

39.   Youngjermchan P, Pumpaisanchai S, Ratchanon S, Pansin P, Tosukhowong P, Tungsanga K, et al. Hypocitraturia and hypokaliuria: major metabolic risk factors for kidney stone disease. 2006.

40.   Sandersius S, Rez PJUr. Morphology of crystals in calcium oxalate monohydrate kidney stones. 2007;35(6):287-93.

41.   Boonla CJROSiLC. Oxidative Stress in Urolithiasis. 2018:129.

42.   Balaban RS, Nemoto S, Finkel TJc. Mitochondria, oxidants, and aging. 2005;120(4):483-95.

43.   Staniek K, Nohl HJBeBA-B. Are mitochondria a permanent source of reactive oxygen species? 2000;1460(2-3):268-75.

44.   Haynes CM, Titus EA, Cooper AAJMc. Degradation of misfolded proteins prevents ER-derived oxidative stress and cell death. 2004;15(5):767-76.

45.   He Y-Y, Häder D-PJJoP, Biology PB. UV-B-induced formation of reactive oxygen species and oxidative damage of the cyanobacterium Anabaena sp.: protective effects of ascorbic acid and N-acetyl-L-cysteine. 2002;66(2):115-24.

46.   Sies HJRb. Oxidative stress: a concept in redox biology and medicine. 2015;4:180-3.

47.   Sies HJCOiT. On the history of oxidative stress: Concept and some aspects of current development. 2018;7:122-6.

48.   Romano AD, Serviddio G, De Mattheis A, Bellanti F, Vendemiale GJJon. Oxidative stress and aging. 2010;23:S29-36.

49.   Shih DM, Xia Y-R, Wang X-P, Miller E, Castellani LW, Subbanagounder G, et al. Combined serum paraoxonase knockout/apolipoprotein E knockout mice exhibit increased lipoprotein oxidation and atherosclerosis. 2000;275(23):17527-35.

50.   Uttara B, Singh AV, Zamboni P, Mahajan RJCn. Oxidative stress and neurodegenerative diseases: a review of upstream and downstream antioxidant therapeutic options. 2009;7(1):65-74.

51.   Kim GH, Kim JE, Rhie SJ, Yoon SJEn. The role of oxidative stress in neurodegenerative diseases. 2015;24(4):325-40.

52.   Liu Z, Zhou T, Ziegler AC, Dimitrion P, Zuo LJOm, longevity c. Oxidative stress in neurodegenerative diseases: from molecular mechanisms to clinical applications. 2017;2017.

53.   Kryston TB, Georgiev AB, Pissis P, Georgakilas AGJMRF, Mutagenesis MMo. Role of oxidative stress and DNA damage in human carcinogenesis. 2011;711(1-2):193-201.

54.   Bhattacharyya A, Chattopadhyay R, Mitra S, Crowe SEJPr. Oxidative stress: an essential factor in the pathogenesis of gastrointestinal mucosal diseases. 2014;94(2):329-54.

55.   Kaltschmidt B, Sparna T, Kaltschmidt CJA, signaling r. Activation of NF-**K** B by reactive oxygen intermediates in the nervous system. 1999;1(2):129-44.

56.   Hoesel B, Schmid JAJMc. The complexity of NF-**K**B signaling in inflammation and cancer. 2013;12(1):1-15.

57.   Roberto P, Giuseppe B, Gabriella SMJA, Signaling R. NF-kappaB: a stress-regulated switch for cell survival. 2006.

58.   Battaglia V, Shields CD, Murray-Stewart T, Casero RAJAa. Polyamine catabolism in carcinogenesis: potential targets for chemotherapy and chemoprevention. 2014;46(3):511-9.

59.   Dizdaroglu MJMRD. Oxidative damage to DNA in mammalian chromatin. 1992;275(3-6):331-42.

60.   Guyton K, Kensler TWJBmb. Oxidative mechanisms in carcinogenesis. 1993;49(3):523-44.

61.   Feig DI, Reid TM, Loeb LAJCr. Reactive oxygen species in tumorigenesis. 1994;54(7 Supplement):1890s-4s.

62.   Beckman KB, Ames BNJPr. The free radical theory of aging matures. 1998.

63.   Khaskhali MH, Byer KJ, Khan SRJUr. The effect of calcium on calcium oxalate monohydrate crystal-induced renal epithelial injury. 2009;37(1):1-6.

64.   Aihara K, Byer KJ, Khan SRJKI. Calcium phosphate–induced renal epithelial injury and stone formation: Involvement of reactive oxygen species. 2003;64(4):1283-91.

65.   Khan SRJJoC, Nephrology E. Crystal-induced inflammation of the kidneys: results from human studies, animal models, and tissue-culture studies. 2004;8(2):75-88.

66.   Khan SRJTa, urology. Reactive oxygen species, inflammation and calcium oxalate nephrolithiasis. 2014;3(3):256.

67.   Boonla C, Wunsuwan R, Tungsanga K, Tosukhowong PJUr. Urinary 8-hydroxydeoxyguanosine is elevated in patients with nephrolithiasis. 2007;35(4):185-91.

68.   Kittikowit W, Waiwijit U, Boonla C, Ruangvejvorachai P, Pimratana C, Predanon C, et al. Increased oxidative DNA damage seen in renal biopsies adjacent stones in patients with nephrolithiasis. 2014;42(5):387-94.

69.   Cooke MS, Lunec J, Evans MDJFRB, Medicine. Progress in the analysis of urinary oxidative DNA damage. 2002;33(12):1601-14.

70.   Boonla C, Krieglstein K, Bovornpadungkitti S, Strutz F, Spittau B, Predanon C, et al. Fibrosis and evidence for epithelial-mesenchymal transition in the kidneys of patients with staghorn calculi. 2011;108(8):1336-45.

71.   Chakhparonian M, Wellinger RJJTiG. Telomere maintenance and DNA replication: how closely are these two connected? 2003;19(8):439-46.

72.   Blasco MAJNRG. Telomeres and human disease: ageing, cancer and beyond. 2005;6(8):611-22.

73.   Von Zglinicki TJTibs. Oxidative stress shortens telomeres. 2002;27(7):339-44.

74.   Harrington LJCoig, development. Those dam-aged telomeres! 2004;14(1):22-8.

75.   Blackburn EHJN. Structure and function of telomeres. 1991;350(6319):569-73.

76.   Smogorzewska A, de Lange TJArob. Regulation of telomerase by telomeric proteins. 2004;73(1):177-208.

77.   Houben JM, Moonen HJ, van Schooten FJ, Hageman GJJFrb, medicine. Telomere length assessment: biomarker of chronic oxidative stress? 2008;44(3):235-46.

78.   Bürkle A, Brabeck C, Diefenbach J, Beneke SJTijob, biology c. The emerging role of poly (ADP-ribose) polymerase-1 in longevity. 2005;37(5):1043-53.

79.   Smith S, Giriat I, Schmitt A, De Lange TJS. Tankyrase, a poly (ADP-ribose) polymerase at human telomeres. 1998;282(5393):1484-7.

80.   Cook BD, Dynek JN, Chang W, Shostak G, Smith SJM, biology c. Role for the related poly (ADP-Ribose) polymerases tankyrase 1 and 2 at human telomeres. 2002;22(1):332-42.

81.   Maestroni L, Matmati S, Coulon SJG. Solving the telomere replication problem. 2017;8(2):55.

82.   Autexier C, Lue NFJARB. The structure and function of telomerase reverse transcriptase. 2006;75:493-517.

83.   Greider CWJArob. Telomere length regulation. 1996;65(1):337-65.

84.   Dong CK, Masutomi K, Hahn WCJCrioh. Telomerase: regulation, function and transformation. 2005;54(2):85-93.

85.   Fakhoury J, Nimmo GA, Autexier CJA-CAiMC. Harnessing telomerase in cancer therapeutics. 2007;7(4):475-83.

86.   Kim NW, Piatyszek MA, Prowse KR, Harley CB, West MD, Ho PdL, et al. Specific association of human telomerase activity with immortal cells and cancer. 1994;266(5193):2011-5.

87.   Harley CB, Futcher AB, Greider CWJN. Telomeres shorten during ageing of human fibroblasts. 1990;345(6274):458-60.

88.   Shawi M, Autexier CJMoa, development. Telomerase, senescence and ageing. 2008;129(1-2):3-10.

89.   Pusceddu I, Farrell C-JL, Di Pierro AM, Jani E, Herrmann W, Herrmann MJCC, et al. The role of telomeres and vitamin D in cellular aging and age-related diseases. 2015;53(11):1661-78.

90.   Makarov VL, Hirose Y, Langmore JPJC. Long G tails at both ends of human chromosomes suggest a C strand degradation mechanism for telomere shortening. 1997;88(5):657-66.

91.   Wright WE, Tesmer VM, Huffman KE, Levene SD, Shay JWJG, development. Normal human chromosomes have long G-rich telomeric overhangs at one end. 1997;11(21):2801-9.

92.   von Zglinicki T, Saretzki G, Döcke W, Lotze CJEcr. Mild hyperoxia shortens telomeres and inhibits proliferation of fibroblasts: a model for senescence? 1995;220(1):186-93.

93.   Vaziri H, West MD, Allsopp RC, Davison TS, Wu YS, Arrowsmith CH, et al. ATM-dependent telomere loss in aging human diploid fibroblasts and DNA damage lead to

the post-translational activation of p53 protein involving poly (ADP-ribose) polymerase. 1997;16(19):6018-33.

94.   von Zglinicki T, Pilger R, Sitte NJFRB, Medicine. Accumulation of single-strand breaks is the major cause of telomere shortening in human fibroblasts. 2000;28(1):64-74.

95.   Kawanishi S, Oikawa SJAotNYAoS. Mechanism of telomere shortening by oxidative stress. 2004;1019(1):278-84.

96.   Sitte N, Saretzki G, von Zglinicki TJFRB, Medicine. Accelerated telomere shortening in fibroblasts after extended periods of confluency. 1998;24(6):885-93.

97.   Petersen S, Saretzki G, von Zglinicki TJEcr. Preferential accumulation of single-stranded regions in telomeres of human fibroblasts. 1998;239(1):152-60.

98.   Ohki R, Ishikawa FJNar. Telomere-bound TRF1 and TRF2 stall the replication fork at telomeric repeats. 2004;32(5):1627-37.

99.   Richter T, Saretzki G, Nelson G, Melcher M, Olijslagers S, von Zglinicki TJMoa, et al. TRF2 overexpression diminishes repair of telomeric single-strand breaks and accelerates telomere shortening in human fibroblasts. 2007;128(4):340-5.

100.   Ju Z, Rudolph K. Telomeres and telomerase in stem cells during aging and disease. Genome and Disease. 1: Karger Publishers; 2006. p. 84-103.

101.   Westhoff JH, Schildhorn C, Jacobi C, Hömme M, Hartner A, Braun H, et al. Telomere shortening reduces regenerative capacity after acute kidney injury. 2010;21(2):327-36.

102.   Hayflick L, Moorhead PS. The serial cultivation of human diploid cell strains. Experimental Cell Research. 1961;25(3):585-621.

103.   Kuilman T, Michaloglou C, Mooi WJ, Peeper DS. The essence of senescence. Genes Dev. 2010;24(22):2463-79.

104.   Campisi J. Aging, tumor suppression and cancer: High wire-act! Mechanisms of ageing and development. 2005;126:51-8.

105.   di Fagagna FdAJNRC. Living on a break: cellular senescence as a DNA-damage response. 2008;8(7):512-22.

106.   Di Leonardo A, Linke SP, Clarkin K, Wahl GMJG, development. DNA damage triggers a prolonged p53-dependent G1 arrest and long-term induction of Cip1 in normal human fibroblasts. 1994;8(21):2540-51.

107.   Wang X, Wong SC, Pan J, Tsao S, Fung KH, Kwong DL, et al. Evidence of cisplatin-induced senescent-like growth arrest in nasopharyngeal carcinoma cells. 1998;58(22):5019-22.

108.   Chang B-D, Xuan Y, Broude EV, Zhu H, Schott B, Fang J, et al. Role of p53 and p21 waf1/cip1 in senescence-like terminal proliferation arrest induced in human tumor cells by chemotherapeutic drugs. 1999;18(34):4808-18.

109.   Berns AJCC. Senescence: a companion in chemotherapy? 2002;1(4):309-11.

110.   Schmitt CA, Fridman JS, Yang M, Lee S, Baranov E, Hoffman RM, et al. A senescence program controlled by p53 and p16INK4a contributes to the outcome of cancer therapy. 2002;109(3):335-46.

111.   te Poele RH, Okorokov AL, Jardine L, Cummings J, Joel SPJCr. DNA damage is able to induce senescence in tumor cells in vitro and in vivo. 2002;62(6):1876-83.

112.   Roninson IBJCr. Tumor cell senescence in cancer treatment. 2003;63(11):2705-15.

113.   Toussaint O, Dumont P, Remacle J, Dierick JF, Pascal T, Frippiat C, et al. Stress-induced premature senescence or stress-induced senescence-like phenotype: one in vivo reality, two possible definitions? ScientificWorldJournal. 2002;2:230-47.

114.   Dimri GP, Lee X, Basile G, Acosta M, Scott G, Roskelley C, et al. A biomarker that identifies senescent human cells in culture and in aging skin in vivo. 1995;92(20):9363-7.

115.   Yang G, Rosen DG, Zhang Z, Bast RC, Mills GB, Colacino JA, et al. The chemokine growth-regulated oncogene 1 (Gro-1) links RAS signaling to the senescence of stromal fibroblasts and ovarian tumorigenesis. 2006;103(44):16472-7.

116.   Lee BY, Han JA, Im JS, Morrone A, Johung K, Goodwin EC, et al. Senescence-associated β-galactosidase is lysosomal β-galactosidase. 2006;5(2):187-95.

117.   Pati S, Jain S, Behera M, Acharya AP, Panda SK, Senapati SJJons, biology,, et al. X-gal staining of canine skin tissues: A technique with multiple possible applications. 2014;5(2):245.

118.   Kawano H, Katsurabayashi S, Kakazu Y, Yamashita Y, Kubo N, Kubo M, et al. Long-term culture of astrocytes attenuates the readily releasable pool of synaptic vesicles. 2012;7(10):e48034.

119.   Choi J, Shendrik I, Peacocke M, Peehl D, Buttyan R, Ikeguchi EF, et al. Expression of senescence-associated beta-galactosidase in enlarged prostates from men with benign prostatic hyperplasia. 2000;56(1):160-6.

120.   Matsunaga H, Handa JT, Aotaki-Keen A, Sherwood SW, West MD, Hjelmeland LMJIo, et al. Beta-galactosidase histochemistry and telomere loss in senescent retinal pigment epithelial cells. 1999;40(1):197-202.

121.   Herbig U, Ferreira M, Condel L, Carey D, Sedivy JMJS. Cellular senescence in aging primates. 2006;311(5765):1257-.

122.   Minamino T, Miyauchi H, Yoshida T, Ishida Y, Yoshida H, Komuro IJC. Endothelial cell senescence in human atherosclerosis: role of telomere in endothelial dysfunction. 2002;105(13):1541-4.

123.   Cristofalo VJ, Lorenzini A, Allen R, Torres C, Tresini MJMoa, development. Replicative senescence: a critical review. 2004;125(10-11):827-48.

124.   Foreman KE, Tang JJEg. Molecular mechanisms of replicative senescence in endothelial cells. 2003;38(11-12):1251-7.

125.   Zhou H, Kato A, Yasuda H, Miyaji T, Fujigaki Y, Yamamoto T, et al. The induction of cell cycle regulatory and DNA repair proteins in cisplatin-induced acute renal failure. 2004;200(2):111-20.

126.   Westhoff JH, Hilgers KF, Steinbach MP, Hartner A, Klanke B, Amann K, et al. Hypertension induces somatic cellular senescence in rats and humans by induction of cell cycle inhibitor p16 INK4a. 2008;52(1):123-9.

127.   Kitada K, Nakano D, Ohsaki H, Hitomi H, Minamino T, Yatabe J, et al. Hyperglycemia causes cellular senescence via a SGLT2-and p21-dependent pathway in proximal tubules in the early stage of diabetic nephropathy. 2014;28(5):604-11.

128.   Glassock RJ, Winearls CJTotAC, Association C. Ageing and the glomerular filtration rate: truths and consequences. 2009;120:419.

129.   Yang L, Besschetnova TY, Brooks CR, Shah JV, Bonventre JVJNm. Epithelial cell cycle arrest in G2/M mediates kidney fibrosis after injury. 2010;16(5):535-43.

130.   Bonventre JVJKis. Primary proximal tubule injury leads to epithelial cell cycle arrest, fibrosis, vascular rarefaction, and glomerulosclerosis. 2014;4(1):39-44.

131.   Wills LP, Schnellmann RGJJotASoN. Telomeres and telomerase in renal health. 2011;22(1):39-41.

132.   Spyridopoulos I, Haendeler J, Urbich C, Brummendorf TH, Oh H, Schneider MD, et al. Statins enhance migratory capacity by upregulation of the telomere repeat-binding factor TRF2 in endothelial progenitor cells. 2004;110(19):3136-42.

133.   Haendeler J, Hoffmann Jr, Diehl JF, Vasa M, Spyridopoulos I, Zeiher AM, et al. Antioxidants inhibit nuclear export of telomerase reverse transcriptase and delay replicative senescence of endothelial cells. 2004;94(6):768-75.

134.   Wang H, Ni J, Guo X, Zhou T, Ma X, Xue J, et al. Shelterin differentially respond to oxidative stress induced by TiO2-NPs and regulate telomere length in human hepatocytes and hepatocarcinoma cells in vitro. 2018;503(2):697-702.

135.   Morekrong P. Epigenetic Regulation of Cellular Aging Induced by Calcium Oxalate Crystals and Naphrolithiasis Urine in HK-2 cells. Thailand: Chulalongkorn University.

136.   Abete P, Napoli C, Santoro G, Ferrara N, Tritto I, Chiariello M, et al. Age-related decrease in cardiac tolerance to oxidative stress. Journal of molecular and cellular cardiology. 1999;31(1):227-36.

137.   Siti HN, Kamisah Y, Kamsiah J. The role of oxidative stress, antioxidants and vascular inflammation in cardiovascular disease (a review). Vascular pharmacology. 2015;71:40-56.

138.   Coyle CH, Martinez LJ, Coleman MC, Spitz DR, Weintraub NL, Kader KN. Mechanisms of H2O2-induced oxidative stress in endothelial cells. Free Radical Biology and Medicine. 2006;40(12):2206-13.

139.   Khaskhali MH, Byer KJ, Khan SR. The effect of calcium on calcium oxalate monohydrate crystal-induced renal epithelial injury. Urological Research. 2009;37(1):1-6.

140.   Satriano J, Mansoury H, Deng A, Sharma K, Vallon V, Blantz R, et al. Transition of kidney tubule cells to a senescent phenotype in early experimental diabetes. American journal of physiology Cell physiology. 2010;299:C374-80.

141.   Liu J, Yang J-R, He Y-N, Cai G-Y, Zhang J-G, Lin L-R, et al. Accelerated senescence of renal tubular epithelial cells is associated with disease progression of patients with immunoglobulin A (IgA) nephropathy. 2012;159(6):454-63.

142.   Satoh M, Ishikawa Y, Takahashi Y, Itoh T, Minami Y, Nakamura M. Association between oxidative DNA damage and telomere shortening in circulating endothelial progenitor cells obtained from metabolic syndrome patients with coronary artery disease. Atherosclerosis. 2008;198(2):347-53.

143.   Kittikowit W, Waiwijit U, Boonla C, Ruangvejvorachai P, Pimratana C, Predanon C, et al. Increased oxidative DNA damage seen in renal biopsies adjacent stones in patients with nephrolithiasis. Urolithiasis. 2014;42(5):387-94.

144.   Schmutz I, de Lange TJCB. Shelterin. 2016;26(10):R397-R9.

145.   Xin H, Liu D, Songyang ZJGb. The telosome/shelterin complex and its functions. 2008;9(9):1-7.

146.   Kishi S, Zhou XZ, Ziv Y, Khoo C, Hill DE, Shiloh Y, et al. Telomeric protein Pin2/TRF1 as an important ATM target in response to double strand DNA breaks. 2001;276(31):29282-91.

147.   van Overbeek M, de Lange TJCb. Apollo, an Artemis-related nuclease, interacts with TRF2 and protects human telomeres in S phase. 2006;16(13):1295-302.

148.   Lei M, Podell ER, Cech TRJNs, biology m. Structure of human POT1 bound to telomeric single-stranded DNA provides a model for chromosome end-protection. 2004;11(12):1223-9.

149.   Yoshimura A, Taira T, Ideura TJEn. Expression of apoptosis-related molecules in acute renal injury. 1996;4(1):15.

150.   Vanijajiva K. Effects of urines from nephrolithiasis patients before and after 6-months treatment with lime powder regimen on oxidative stress and inflammation in renal tubular cells Thailand: Chulalongkorn university; 2013.

151.   Furukawa A, Tada-Oikawa S, Kawanishi S, Oikawa S. H2O2 accelerates cellular senescence by accumulation of acetylated p53 via decrease in the function of SIRT1 by NAD+ depletion. Cellular physiology and biochemistry : international journal of experimental cellular physiology, biochemistry, and pharmacology. 2007;20(1-4):45-54.

152.   Zdanov S, Remacle J, Toussaint O. Establishment of H2O2-induced premature senescence in human fibroblasts concomitant with increased cellular production of H2O2. Annals of the New York Academy of Sciences. 2006;1067:210-6.

153.   Suo R, Zhao Z-Z, Tang Z-H, Ren Z, Liu X, Liu L-S, et al. Hydrogen sulfide prevents H2O2-induced senescence in human umbilical vein endothelial cells through SIRT1 activation. Mol Med Rep. 2013;7(6):1865-70.

154.   Oeseburg H, Iusuf D, van der Harst P, van Gilst WH, Henning RH, Roks AJJH. Bradykinin protects against oxidative stress–induced endothelial cell senescence. 2009;53(2):417-22.

155.   Small DM, Bennett NC, Roy S, Gabrielli BG, Johnson DW, Gobe GC. Oxidative Stress and Cell Senescence Combine to Cause Maximal Renal Tubular Epithelial Cell Dysfunction and Loss in an in vitro Model of Kidney Disease. Nephron Experimental Nephrology. 2012;122(3-4):123-30.

156.   Baggio B, Gambaro G, Ossi E, Favaro S, Borsatti AJTJou. Increased urinary excretion of renal enzymes in idiopathic calcium oxalate nephrolithiasis. 1983;129(6):1161-2.

157.   Tungsanga K, Sriboonlue P, Futrakul P, Yachantha C, Tosukhowong PJUr. Renal tubular cell damage and oxidative stress in renal stone patients and the effect of potassium citrate treatment. 2005;33(1):65-9.

158.   Selvam RJUr. Calcium oxalate stone disease: role of lipid peroxidation and antioxidants. 2002;30(1):35-47.

159.   Thamilselvan S, Byer KJ, Hackett RL, Khan SRJTJou. Free radical scavengers, catalase and superoxide dismutase provide protection from oxalate-associated injury to LLC-PK1 and MDCK cells. 2000;164(1):224-9.

160.   Khaskhali MH, Byer KJ, Khan SR. The effect of calcium on calcium oxalate monohydrate crystal-induced renal epithelial injury. Urol Res. 2009;37(1):1-6.

161.   Aihara K, Byer KJ, Khan SR. Calcium phosphate-induced renal epithelial injury and stone formation: involvement of reactive oxygen species. Kidney Int. 2003;64(4):1283-91.

162. Chen QM, Prowse KR, Tu VC, Purdom S, Linskens MHK. Uncoupling the Senescent Phenotype from Telomere Shortening in Hydrogen Peroxide-Treated Fibroblasts. Experimental Cell Research. 2001;265(2):294-303.

163. Palm W, de Lange TJArog. How shelterin protects mammalian telomeres. 2008;42:301-34.

164. Opresko PL, Fan J, Danzy S, Wilson III DM, Bohr VAJNar. Oxidative damage in telomeric DNA disrupts recognition by TRF1 and TRF2. 2005;33(4):1230-9.

165. Van Steensel B, De Lange TJN. Control of telomere length by the human telomeric protein TRF1. 1997;385(6618):740-3.

166. Okamoto K, Bartocci C, Ouzounov I, Diedrich JK, Yates III JR, Denchi ELJN. A two-step mechanism for TRF2-mediated chromosome-end protection. 2013;494(7438):502-5.

167. Rice C, Shastrula PK, Kossenkov AV, Hills R, Baird DM, Showe LC, et al. Structural and functional analysis of the human POT1-TPP1 telomeric complex. 2017;8(1):1-13.
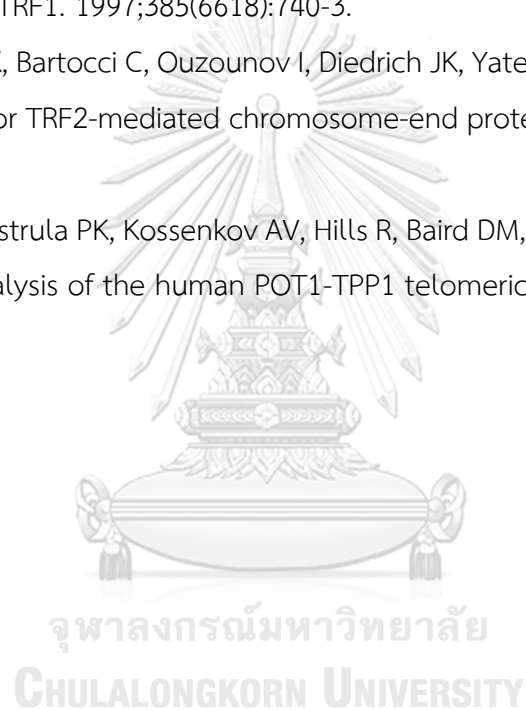
REFERENCES

VITA

NAME	Miss Kamonchanok Chuenwisad
DATE OF BIRTH	29 July 1991
PLACE OF BIRTH	Surat Thani
INSTITUTIONS ATTENDED	Faculty of Medicine Siriraj Hospital, Mahidol University
HOME ADDRESS	Surat Thani, Thailand

จุฬาลงกรณ์มหาวิทยาลัย
CHULALONGKORN UNIVERSITY